Vertical profiles of O_3, aerosols, CO and NMHCs in the Northeast Pacific during the TRACE-P and ACE-ASIA experiments

Heather U. Price[1, 2], Daniel A. Jaffe[2], Paul V. Doskey[3], Ian McKendry[4], and Theodore L. Anderson[5]

[1]Department of Chemistry, University of Washington, Seattle WA 98195, Tel: 425-352-3264, Fax: 425-352-5233, Email: hprice@u.washington.edu

[2]Interdisciplinary Arts and Sciences, University of Washington, Bothell WA, 98011-8246. Tel: 425-352-5357, Fax: 425-352-5233, Email: djaffe@u.washington.edu

[3] Environmental Research Division, Argonne National Laboratory, Argonne Illinois 60439, Tel: 630-252-7662; Fax: 630-252-5498, Email: pvdoskey@anl.gov

[4]Department of Geography, University of British Columbia, 251-1984 West Mall, Vancouver, B.C. Canada, V6T 1Z2. Tel: 604-822-4929; Fax: 604-822-6150, Email: ian@geog.ubc.ca

[5]Atmospheric Sciences, University of Washington-Seattle, Seattle WA 98195, Tel: 206-543-2044, Fax: 206-543-0308, Email: tadand@atmos.washington.edu

Accepted January 2003

ABSTRACT

Airborne observations of NMHCs, O_3, CO and aerosol scatter were made near the coast of Washington State from 29 March to 6 May 2001 as part of the Photochemical Ozone Budget of the Eastern North Pacific-II (PHOBEA-II) experiment. These observations overlapped the time period of the TRACE-P (24 February to April 10, 2001) and ACE-ASIA (27 March to 30 April, 2001) experiments operating in the Western Pacific. Measurements were made during 12 flights at 48.31±0.03°N latitude, 124.63±0.08°W longitude at altitudes from 0-6km. On several flights significant enhancements in all species were observed and are attributed to transport from the Eurasian continent, including a long-range transport event observed on 14 April 2001. This event contained substantial CO, NMHC and aerosol loadings and was identified by the Total Ozone Mapping Spectrometer (TOMS) aboard the Earth Probe Satellite, and airborne and surface measurements throughout North America. This airmass was unique in that it contained the highest levels of aerosol scatter, CO, and various NMHCs observed in 2001, was the only flight with a low Ångstrom coefficient (0.7) indicating dominance of super micron aerosols, and had a negative relationship between ozone and aerosol scatter (r = -0.30). Within this mineral dust and pollution layer, aerosol scatter, propane and CO were enhanced by 1054%, 85% and 36%, respectively, over the observed spring 2001 median values between 3.5 and 6 km. A comparison of our previous aircraft campaign, in 1999, with 2001 observations shows that ozone, aerosol scatter and most NMHCs were significantly lower in the spring of 2001. The exact cause is still under investigation, but the combination of elevated ozone, aerosol scatter and NMHCs suggests a combustion source that was enhanced and/or transported more efficiently during the spring of 1999.

1. INTRODUCTION

Throughout East Asia increases in emissions from transportation, biomass burning and power sources have paralleled unprecedented economic and industrial growth [*Kato and Akimoto, 1992; Akimoto and Narita, 1994; van Aardenne et al., 1999; Streets and Waldhoff, 2000*]. For instance, since the mid-1970s East Asian emissions of NOx and SO_2 have increased 5% yr^{-1} reflecting increases in fossil fuel energy use [*Kato and Akimoto, 1992*]. Such increases are expected to continue until at least 2015, resulting in a doubling of NO_x emissions within 15 years. Global models suggest that this NO_x increase will increase ozone in the Western United States [*Berntsen et al., 1999, IPCC 2001a, Jacob et al., 1999*].

A number of models and observations have studied the outflow of Eurasian pollution to the western and central North Pacific [*Gregory et al., 1996; Jaffe et al., 1997; Ridley et al., 1997; Talbot et al., 1997; Phadnis and Carmichael, 2000; Kato et al., 2001*]. Additional studies suggest anthropogenic pollutants emitted on the Eurasian continent can impact trace gas concentrations and photochemistry along the West Coast of the US [*Parrish et al., 1992; Andreae et al., 1988; Jaffe et al., 1999; Bailey et al., 2000; Jaffe et al., 2001; Kotchenruther et al., 2001*]. According to one global chemical transport model (GCTM) [*Fiore et al., 2002*] anthropogenic emissions in Asia and Europe increase afternoon O_3 concentrations in surface air over the U.S. by 4-7 ppbv, both under average and highly polluted conditions.

Pollutants emitted from northern midlatitude continents including North America, Europe and Asia, are delivered to the North Pacific by circumpolar westerly transport. From fall through spring, midlatitude westerlies dominate flow over the North Pacific.

The Aleutian low and Pacific high together direct the strongest midlatitude westerly flow into the western United States.

During the Photochemical Ozone Budget of the Eastern North Pacific (PHOBEA-I) field campaign measurements of carbon monoxide (CO), ozone (O_3), aerosols and nitrogen oxides (NOx) were made during the springs of 1997-1999 at both Cheeka Peak Observatory (CPO) and from the University of Wyoming King Air research aircraft [*Jaffe et al., 2001; Kotchenruther et al., 2001*]. CPO observations showed evidence for the transport of emissions from the Eurasian region to the western United States in as little as six days [*Jaffe et al., 1999*]. Since the 1997 event, additional long range transport (LRT) events to North America have been observed [*Jaffe et al., 2003*]. The airborne measurements showed several episodes of enhanced pollutants originating from the Eurasian continent that contained enhanced nonmethane hydrocarbons (NMHCs), peroxyacetyl nitrate (PAN), aerosols and O_3 to a maximum value of 90ppbv [*Kotchenruther et al., 2001*]. However, not all LRT events contained elevated O_3 [*Jaffe et al., 2003*].

The 2001 PHOBEA field campaign, off the coast of Washington State, provided an opportunity to sample in the Northeast Pacific at the same time that two major field studies were underway in the Western Pacific: the Transport and Chemical Evolution over the Pacific (TRACE-P) [*Jacob et al., this issue*] and Asia-Pacific Regional Aerosol Characterization Experiment (ACE-ASIA) [*Huebert et al., 2002*]. This meant that an unprecedented suite of observations were conducted simultaneously in the North Pacific. Furthermore, several GCTMs were exploited. The overall objectives of PHOBEA were to identify sources, correlations, patterns and relationships between species observed over the Northeast Pacific during spring of 2001. In this paper we present the results of

vertical airborne measurements of CO, O_3, NMHC and aerosol scatter made during this project and seek to answer the following questions.

1. What is the relationship among the measured species and what does this tell us about sources?
2. What is the interannual variability and controlling factors for lower overall pollutant mixing ratios observed during 2001 in the Northeast Pacific?
3. How well do GCTMs reproduce the PHOBEA observations and
4. Using the combination of the observation and a GCTM what are the sources and sinks for CO and O_3 in the Northeast Pacific.

In this paper we focus on the first two questions and the companion paper by *Jaeglé et al.* [this issue] addresses the last two questions.

2. EXPERIMENTAL

Measurements were made from a Beechcraft Duchess aircraft on 12 flights from March 29 to May 6, 2001 (day of year (DOY) 89 to 125). Specific flight dates and sampling start times are listed in Table 1. The Duchess is a twin engine (piston) aircraft, which can reach 6 km altitude, can carry approximately 200kg of sampling equipment and can provide approximately 1 kwatt of 28vdc power. All vertical profiles were conducted in the vicinity of CPO near the northwest corner of Washington State at 48.31 ± 0.03 ° N latitude, 124.63 ± 0.08° W longitude and at altitudes between 0-6km.

The aircraft was based out of Paine Field in Everett, Washington, 30 miles north of Seattle. A typical research flight took place in daylight and lasted roughly 3 hours. Instruments were turned on shortly before take-off, warmed up and zeroed during the 45-minute ferry leg to the sampling area off the Washington Coast. Before landing at Paine Field, all instruments were turned off.

Flight days were chosen using several methods to minimize local North American pollution and obtain representative samples of Pacific air. For this purpose we used predicted wind fields, backward and forward trajectory analysis from NOAA's Hybrid Single-Particle Lagrangian Integrated Trajectory (HYSPLIT) Model, the GEOS-Chem chemical transport model run in forecast mode and satellite observations of aerosol index from TOMS [*Jaeglé et al., this issue; Jacob et al., this issue*].

GEOS-Chem is a global three-dimensional model of tropospheric chemistry driven by assimilated meteorology from the Goddard Earth Observing System (GEOS) of the NASA Data Assimilation Office. The model considers six tagged CO source regions: (1) North America, (2) Asia, (3) Europe, (4) CH_4 + VOC oxidation and (6) others. *Bey et al*. [2001] provides a detailed description of the model and a comparison to 2001 PHOBEA observations can be found in *Jaeglé et al.* [this issue]. While it is possible that using these forecast products might bias our flight days toward LRT episodes we tried to avoid this. A comparison of these 12 flights with GCTM results from the entire period suggests that our data are representative of the entire time period [*Jaeglé et al., this issue*].

The Duchess aircraft was outfitted as shown in Figure 1 with sensors to measure ozone, aerosol light scattering, temperature, pressure, relative humidity, and canisters for CO and NMHCs. Raw analog data for ozone, aerosol scatter, temperature, relative humidity and pressure were collected at a rate of 1Hz using a Toshiba laptop computer through a PCMIA data acquisition card (PCM-CIA16D/16; Computer Boards, Inc., Middleboro, MA). Data collection through the card was controlled by Labtech Notebookpro® software. A global positioning unit collected latitude, longitude, and altitude parameters at a rate of 0.2 Hz to internal memory, which was later downloaded and integrated with the 1 Hz analog data.

Whole air samples, pressurized to 1000-1700 hPa, were collected at various altitudes in stainless steel canisters and later analyzed for CO at the University of Washington-Bothell by reduction gas analysis and for NMHCs at Argonne National Laboratory by cryogenic preconcentration/high-resolution gas chromatography, [*Doskey and Gaffney, 1992*]. Canister samples were collected at altitudes of 6, 5, 4, 3, 2, and 0.5 km during which a constant altitude was maintained for 2-5 minutes. Additional canister samples were collected if a substantial pollution layer was identified from the aerosol scattering data.

Samples were collected from two rear facing stainless steel inlets situated forward of and above the wing-mounted engines. The inlets were built into a plexiglass plate, which was bolted into the pilot's side window. For the canister samples we used a ¼" o.d., 3/16" i.d. Silcosteel (Restek Inc.) inlet and 2 meters of ¼" o.d., 3/16" i.d. stainless tubing. The ozone and nephelometer sampled from a common ¼" o.d., 3/16" i.d. stainless steel inlet, which branched just inside the aircraft to the two instruments. Sampling lines inside the plane consisted of 1.5 meters of ¼" o.d., 3/16" i.d. Teflon (PFA) tubing for ozone and 2 meters of ¼" o.d., 3/16" i.d. stainless steel for the aerosol nephelometer.

Ozone was measured using a miniaturized ultraviolet instrument (2B Technologies Ozone Monitor; Golden, CO). *Bognar and Birks* [1996] detail the analytical aspects of the miniaturized ozone instrument. In our version of this instrument we found significant humidity interference, which was eliminated by switching to a quartz optical cell. We calibrated the instrument before, during and after the spring 2001 campaign using a standard ozone calibrator (Columbia Scientific Inc.). To obtain an accurate blank reading for each flight, the instrument was zeroed using a charcoal scrubber during the outgoing ferry leg of each flight, as recommended by *Bognar and Birks* [1996]. This instrument

was intercompared against a Dasibi ozone instrument and an electrochemical cell ozonesonde during the summer of 2001 in the Duchess at altitudes up to 6 km resulting in very close agreement. The ratio of the Dasibi O_3 to 2B O_3 for the summer 2001 data set was 0.99 [*Snow et al., 2002*]. We also examined O_3 loss in the short section of stainless steel inlet and found it to be negligible. This instrument has a higher noise level than the Dasibi, which is reduced by averaging the data to the times of the level flight legs (~5min). The total uncertainty in the ozone measurement for a 1-minute averaging period was 6%.

Aerosol scattering measurements were made through a standard rear facing 0.533 mm i.d. stainless steel inlet using an integrating nephelometer (TSI 3563; Shoreview, MN) at three wavelengths; red (700 nm), green (550 nm), and blue (450 nm). The nephelometer was calibrated with gases of known scattering coefficients (air and CO_2) and has a total uncertainty to scattering coefficients of, the larger of 2.0×10^{-7} m^{-1} or 11 percent, for a 60-second averaging time. Measurements of the calibration gases were made prior to the campaign and zero offsets were determined by sampling filtered air during the outbound ferry leg of each flight.

By using a standard rear-facing inlet, larger particles were excluded from the measurements. Based on a comparison of the Ångstrom exponent (Figure A1) measured during this campaign with Mie scattering theory, we estimate that our aerosol collection cutoff is approximately $0.7 \pm 0.1\mu m$ geometric diameter. Details are given in the appendix. Thus our scattering coefficients approximately represent the sub-micron aerosol scattering. The reported aerosol scattering coefficients are expressed relative to standard pressure and temperature. Except for the discussion on Ångstrom exponent, we use total scattering by particles in the green (σ_{sg}) for our data interpretation.

Water vapor mixing ratios were calculated as a function of pressure, temperature, and relative humidity using the Bolton equation for saturation vapor pressure [*Bolton, 1980*].

A total of 75 whole air samples for CO and NMHCs analysis were collected in evacuated 1.8-liter stainless steel canisters (Scientific Instrumentation Specialists, Moscow, Idaho) for later analysis. A manually operated whole air sampler was designed for use in the Duchess aircraft. The sampler consists of a viton diaphragm pump (model: UN05svi, Neuberger, Inc., Trenton, NJ), a manifold for connecting up to 8 canisters, a pressure gauge and a 2-position valve. Canisters were filled to pressures between 1000-1700 hPa.

The whole-air samples were analyzed for CO at the UW-Bothell and then shipped to Argonne National Laboratory for analysis of NMHCs. Carbon monoxide was analyzed using a standard Reduction Gas Analyzer (RGA) (Trace Analytical, Inc. Model # TA3000), and is referenced to a NIST standard reference material (NIST SRM 2612a). The uncertainty of the NIST standard is 1.7%. Precision of our analysis as determined from replicate measurements over the course of the campaign is 2.1% with a total uncertainty for CO of less than 5%.

Analysis for NMHCs were made on two systems each consisting of a panel-mounted cryofocusing unit and a Hewlett-Packard (HP 5890) high-resolution gas chromatograph with flame ionization detector (GC-FID) [*Doskey and Bialk, 2001*]. One GC-FID system employed a 30m x 0.53mm i.d. porous layer open tubular (PLOT) column coated with alumina (GS-Alumina; J&W Scientific, Folsom, CA) and the other used a 60m x 0.32mm i.d. fused-silica capillary column coated with 1μm-thick film of poly(dimethylsiloxane) (DB-1; J&W Scientific, Folsom, CA).

Calibration of the FIDs took place during each day's analysis using a mixture of C_2-C_6 n-alkanes, benzene and toluene with mixing ratios of 10 ppb each (Scott Specialty Gases, Inc., Plumsteadville, PA). The analytical accuracy of the standard is ±10% and uncertainty of the response factors, determined from replicate injections over the course of analyses, for the PLOT and DB-1 columns are 1.9% and 3.5%, respectively. Measurements of C_3-C_4 alkanes and alkenes are made on both systems to verify the comparability of the two analytical systems.

3. RESULTS

3.1 Meteorology during Spring 2001

Meteorological conditions over the North Pacific during PHOBEA 2001 were examined using the reanalysis data of the National Centers for Environmental Prediction (NCEP) (http://www.ncep.noaa.gov). Conditions during spring 2001 were, in general, similar to the climatological mean (1979-1985), with typical strong zonal flow at 500mb across the North Pacific. During spring 2001 the Pacific high was ~4mb stronger and the center of the Aleutian low was shifted ~5 degrees north compared to the long term mean. A weak La Niña was present in early 2001 in the tropical Pacific but neutral ENSO conditions developed and were maintained throughout the latter half of the year (http://lwf.ncdc.noaa.gov).

3.2 Data Averages

Table 1 gives flight dates, sampling start times, and includes a short description of general air mass types encountered during each flight. In Table 2 we present two columns of vertically binned data averages from the spring 2001 research flights. The first column includes data from all flights while the second column represents only marine data, excluding North American and locally influenced air masses.

A number of air mass types were encountered during the campaign including North American continentally influenced, aged North Pacific, and long-range transport (LRT) from the Eurasian region. A combination of trace gas mixing ratios, backward trajectories and NMHC ratios on per carbon basis, were used to determine the various airmass types. NMHC ratios of ethane/propane and acetylene/CO are indicators of photochemical processing and dilution [*McKeen et al., 1996*]. As an airmass ages these ratios will increase because propane and acetylene react 4.3 and 3.7 times faster with OH than ethane and CO, respectively, and from mixing with background air during transport. A description of each airmass type follows and three case studies detailing several of these are discussed in section 4.

Flights influenced by North American emissions are characterized by backward trajectories that pass over the North American continent, generally high mixing ratios for CO, NMHCs and aerosol scatter, and lower ethane/propane and CO/acetylene ratios. Because of our interest in air masses from the North Pacific and Eurasian regions, altitude segments influenced by North American continental emissions are excluded from the "Marine" data averages in Table 2 and from subsequent analyses. Therefore, the marine data excludes flight 4 below 3.5km and all altitudes of flights 5 and 7. The marine data are also called the "spring 2001 background" in subsequent discussions and represent 82% of the entire dataset.

Aged North Pacific airmasses represent 20% of the dataset. These airmasses are characterized by mixing ratios below the spring 2001 background, backward trajectories suggesting no contact with land for at least 10 days, cycling in the vicinity of the Pacific high, and high ethane/propane and CO/acetylene ratios.

A majority (62%) of the airmasses observed during the PHOBEA 2001 campaign originated over high latitudes and Eurasian continent, hereafter called "Eurasian airmasses". Eurasian airmasses are characterize by elevated mixing ratios of CO and C_2-C_6 NMHCs, and elevated aerosol scattering, which are attributed to LRT of biomass burning, industrial pollution, mineral dust emissions or some combination of these originating from the Eurasian continent. In many cases backward trajectories show transport directly from the Eurasian continent within 10 days and ethane/propane and CO/acetylene ratios roughly between that of aged North Pacific and fresh North American continental airmasses.

Ethane/propane ratios observed during the PHOBEA 2001 experiment for relatively fresh North American influenced, Eurasian, and aged North Pacific airmasses are 2.52 ± 0.70, 2.89 ± 0.55, and 5.54 ± 1.71, respectively (on per carbon basis). Following the same trend, the CO/acetylene ratios are 0.24 ± 0.06, 0.27 ± 0.06, and 0.58 ± 0.20 (on per carbon basis) for North American, Eurasian and aged North Pacific airmasses, respectively. Ethane/propane ratios of fresh Asian continental outflow observed at 0-2km during PEM-West B in spring 1994 and ACE-ASIA on April 8, 2001 (N = 30) have the smallest ratios at 1.62 ± 0.29 and 1.48 ± 0.23 (per carbon), respectively, [*Talbot et al., 1997; T. Chen, personal communications 2002*]. The CO/acetylene ratio observed during PEM-West B follows the trend as well, with a ratio of 0.11 ± 0.02 (per carbon) [*Talbot et al., 1997*].

4. DISCUSSION

4.1 Species Relationships

A linear correlation matrix (*r* values) for select species including data from all flights is presented in Table 3. Correlations are generally similar to those from our previous 1999 aircraft observations [*Kotchenruther et al., 2001*]. Correlations between aerosol scatter and other components, such as C_2-C_6 NMHCs are slightly stronger in 2001. For instance, the correlation coefficient for carbon monoxide with aerosol scatter in 2001 is $r = 0.56$ (N = 56) compared to $r = 0.40$ in 1999 (N = 31). We attribute the stronger correlations of aerosol scatter with CO in 2001 and NMHCs to the significant LRT event observed on April 14, 2001, flight 8 (described below). When this flight is removed, the 2001 correlations for aerosol scatter with CO and C_2-C_6 NMHCs (N = 48) become generally similar to the 1999 *r*-values. For example, when flight 8 is excluded from the correlation of aerosol scatter with CO the correlation coefficient is reduced to 0.32.

The correlation between ozone and aerosol scatter (λ = 550nm) is positive for all flights in 2001 with *r*-values ranging from 0.06-0.86 (N = 79±8), with the exception of flight #8 (April 14, 2001) where $r = -0.30$ (N = 89) (Figure 3). As pollution tends to be transported in vertical layers rather than uniformly it is useful to explore correlations within specific vertical bins. The correlation between ozone and aerosol scatter below 3.5km is $r = 0.62$ (N = 566) and above is $r = 0.10$ (N = 249) for all Marine flights. When the dust event on April 14, 2001 (flight 8) is excluded, these become $r = 0.62$ (N = 506) below 3.5km and $r = 0.44$ (N = 219) above 3.5km. It is important to recall that our aerosol scattering values include only sub-micron aerosols. The positive correlation between ozone and aerosol scatter suggests that, except for flight 8, the observed aerosol

and ozone are associated with the same sources, most likely industrial and/or biomass burning.

4.2 Comparison between 1999 and 2001 PHOBEA aircraft observations

The mixing ratios of natural and anthropogenic species in the PHOBEA research area are not necessarily constant from year to year due to variability in transport and sources. To examine these variations, we conducted a statistical comparison of the 1999 and 2001 PHOBEA aircraft data sets, which were taken at the same time of year. To account for autocorrelation in the one-minute data, each flight was averaged into flight legs with six altitude bins from 0-1.5, 1.5-2.5, 2.5-3.5, 3.5-4.5, 4.5-5.5, and 5.5-6.0 km prior to running the statistical tests. To investigate differences between the two years based on altitude we compared data from 0-3.5 km and 3.5-6 km. Results from the statistical comparison are shown in Table 4. Flights not included in this analysis because they do not reflect the average concentrations observed during the two years are; (1) the observation of a stratospheric intrusion event April 3, 1999 with ozone levels above 300ppbv at 7km and (2) the dust event observed April 14, 2001 containing substantial aerosol loadings and elevated carbon monoxide and hydrocarbons at altitudes above 3.5 km and (3) any flight legs with evidence of recent North American emissions.

Between 3.5-6.0 km nearly all species were elevated in 1999 compared to 2001, with the exception of n-butane and CO, which show essentially no difference. At 0-3.5km the pattern is less clear, where ozone, acetylene, i-pentane and ethane are higher in 1999 but other species are not. Possible controlling factors giving rise to higher concentrations in 1999 may include injection of ozone rich stratospheric air into the troposphere, above average combustion sources in Eurasia, or increased transport of emissions from source regions during 1999 compared to 2001.

Incidence of stratospheric intrusion may have been more frequent or stronger during spring of 1999 compared to 2001, resulting in higher ozone levels observed in 1999. Kotchenruther identified one episode of stratospheric influence in the 1999 data. However, even when this event is excluded the average ozone values are still higher in 1999 compared to 2001. To explore this we looked at a number of variables including tropopause height, potential vorticity, backward trajectories and the correlation between ozone and water vapor in 1999 and 2001.

To explore if the differences in ozone observed in the PHOBEA research area in 1999 [*Kotchenruther et al., 2001*] and 2001 (Table 2) were seen at other west coast locations, we examined ozonesonde data from Trinidad Head, on the North California coast (41.3 N, 124.9 W), about 900 km south of the PHOBEA research area. The Trinidad Head ozonesonde data, shown in figure 4, corroborate our aircraft results that during spring 1999 ozone was significantly higher than 2001.

The mean tropopause pressure (http://www.cdc.noaa.gov) over the North Pacific and NE Asia, between 135-155E and 50-70N, was 20-50mb greater in the spring of 1999, compared with 2001. Because anomalously low tropopause heights are a characteristic of isolated vortices, called cutoff cyclones, it is possible that there were more frequent or more persistent cutoff cyclones during spring of 1999 compared to 2001 [*J. Holton, personal communication 2002; Hoskins et al., 1985*]. Exchange in cutoff cyclones can occur by convective erosion of an anomalously low tropopause and by turbulent mixing associated with tropopause folding along the edges of the system [*Hoskins et al., 1985; Holton et al., 1995*].

Since water vapor is very low in the stratosphere compared with the troposphere, a negative correlation between water vapor and ozone would be expected in airmasses

associated with tropopause folds. The correlation (*r* value) between ozone and water vapor was stronger in 1999 (–0.60) compared to 2001 (-0.45). Thus the stronger correlation between ozone and water vapor in 1999 may reflect greater stratospheric influence or differences in source emissions for ozone between the two years.

To explore if there was more air mass descent during the 1999 campaign, we compared six-day backward trajectories for all flights during 1999 and 2001 ending at 4, 5 and 6km over our research area (not shown). Trajectories were calculated using NOAA's HYSPLIT model and correspond to 14 aircraft flight dates in 1999 and 8 flight dates in 2001, with arrival heights of 4, 5, and 6km [*Draxler and Hess, 1997, 1998*]. Trajectories reaching the aircraft research site at 4-6km arrived from an average of 632 meters higher in 1999 compared to 2001. In addition, the maximum descent of these trajectories averaged 871 meters greater in 1999.

To examine if ozone during 1999 was elevated due to intrusions of stratospheric air, we compared potential vorticity (PV) over the research area during the springs of 1999 and 2001. PV has a direct relationship to ozone variability in the tropopause region, and in the absence of diabatic heating and frictional forces it is a conserved tracer of stratospheric air that has been transported into the troposphere. A study of PV plots for the springs of 1999 and 2001 in the northeast Pacific (not shown) do not suggest a difference in stratospheric influence between the springs of 1999 and 2001.

From our analysis of tropopause heights, backward trajectories, and potential vorticity it is not clear whether elevated O_3 observed during the spring of 1999 compared to 2001 was due to an enhanced stratospheric flux. Higher than average Eurasian combustion emissions, possibly from greater biomass burning emissions in 1999, or differences in emissions or transport may be responsible for the higher mixing ratios of

ozone, NMHCs and aerosols. An especially intense biomass burning season occurred during the spring of 1999 in the Indian subcontinent and SE Asia resulting in biomass burning emissions 30% higher than the 20-year average [*Staudt et al., 2001; Duncan 2002*]. However, if the combustion source during 1999 were from biomass burning we would expect methyl chloride (CH_3Cl) to be also be elevated during 1999. From Table 4 we see that CH_3Cl was not elevated in 1999 compared to 2001. Thus, at this point we cannot determine whether increases in combustion sources or increased transport from source areas in 1999 are responsible for the observed elevated mixing ratios. To determine which of these is responsible, an extensive modeling study using a GCTM will be necessary.

4.2 CASE STUDIES

4.2.1 April 14, 2001 (Flight 8)

The LRT of Eurasian airmasses to North America is generally characterized by frontal lifting of boundary layer air followed by rapid transport across the Pacific within ~7days [*Stohl et al., 2001*]. A strong mid-latitude storm system moved across Mongolia and northeastern China during April 6-8th and produced a massive sandstorm as it crossed the Gobi Desert. Desert dust from this storm mixed with anthropogenic pollution as it passed through the industrial regions of NE Asia. The dust cloud was tracked by the Total Ozone Mapping Spectrometer (TOMS) instrument, onboard the Earthprobe satellite, as it developed in Asia and was transported to North America (Plate 12a and 12b).

A strong frontal system associated with a warm front moved over the Pacific Northwest late on April 12th bringing heavy rain along the Washington coast. Conditions improved on the 13th and 14th with increasing pressure and decreasing rain.

Figure 5 shows the data from April 14 (flight 8), when levels of CO, C_2-C_6 NMHCs and aerosol scatter were the highest observed during the 2001 campaign. Unlike the LRT case of May 6, 2001 (discussed below), where ozone was positively correlated with aerosol scatter, ozone mixing ratios during flight 8 were within 1 standard deviation of the spring 2001 mean and negatively correlated (r = -0.56) with aerosol scatter within the dust and pollution layer (3.5-6.0km). Vertical profiles for ozone, aerosol scatter and water vapor show a rise in aerosol scatter and concurrent decrease in ozone and water vapor beginning at 3.5km and peaking at 4.5-6km. Within the dust layer (3.5-6 km) aerosol scatter and water vapor were 840% higher and 75% lower, respectively, than the average 2001 spring background for that altitude (Table 5).

Ethane and propane within the airmass (3.5-6km) were observed at mixing ratios of 1613 and 462 pptv, 42 and 99 percent higher than the 2001 springtime background mixing ratios of 1133 and 232pptv, respectively. Relatively short-lived gases, including i-butane and toluene also showed high mixing ratios of about 69 and 7 pptv compared to the 2001 background ratios of 25 and 2, respectively. The ethane/propane ratios 2.19 ± 0.13 (on a per carbon basis) observed at 3.5-6km on April 14 is somewhat higher than the ratios of 1.48 ± 0.23 (per carbon) observed in Asian outflow on April 8, 2002 during the ACE-Asia experiment [*T. Chen, personal communication 2002*]. High ratios of ethane relative to propane are caused by faster photochemical removal of propane relative to ethane as well as by mixing with background air during long-range transport, both indicating the air was slightly aged compared to the relatively fresh outflow emissions observed off the Asian continent during ACE-Asia [*McKeen et al., 1996*].

In addition this was the only flight with a negative correlation between ozone and aerosol scatter, with r = 0.66 below 3.5km, -0.56 above 3.5km, and an overall

negative correlation of -0.30 between 0-6km (Figure 3). There are a number of possible reasons for the relative absence of ozone and negative correlation between ozone and aerosol scatter above 3.5km.

Using the scattering coefficient in the red and green we calculate the Ångstrom exponent using equation 1A. The Ångstrom exponent observed at 4.5-6km was 0.7, which is quite different from the Ångstrom exponent observed in most long range transport events (~2.1) [*Jaffe et al., 2003*]. This Ångstrom exponent indicates that the aerosol size distribution was dominated by super-micron mineral dust particles. The fact that the aerosol size distribution on April 14 was dominated by super micron particles means that our measured scattering coefficient for this date significantly underestimates the total aerosol scatter. More details on the calculation of the Ångstrom coefficient are given in the appendix.

The presence of dust probably impacted the production and/or lifetime of ozone in the source region and during transport. One possibility is that ozone was present in the source region but depleted en route. Elevated dust and transport in a dry airmass are both suggested as contributing factors to ozone loss on the dust particles [*Dentener et al., 1996*]. Moreover, indirect evidence by *Galbally and Roy* [1980] suggests that the deposition velocity of ozone on dry sand is approximately two times greater than on wet soils. Another possibility is that ozone was not generated in the source region. Reductions in UV reaching the surface due to large amounts of mineral dust may have prevented ozone from forming [*Dickerson et al., 1997*].

A variety of data sources can be used to understand the transport and sources of the substantial gas and aerosol enhancements observed on April 14, 2001. These include

backward trajectories, TOMS satellite retrievals of absorbing aerosol index, and the GEOS-Chem global chemical transport model.

Backward trajectories (Figure 6) show that the air sampled on April 14 passed over the Gobi desert and industrial regions of Northeast China and the Korean peninsula ~7 days prior to being sampled. Meteorological conditions for April 6 and 7, from NCEP data, show extremely high winds averaging 14-16m/s over the Gobi desert. Such winds are likely responsible for the mobilization and injection of desert dust into the air mass prior to its transport east through the industrial regions of Northeast China and Korea [*Gong et al., 2002*]. It was during transport through these industrial regions where pollutants such as CO and C_2-C_6 NMHCs were introduced. During this time a low was located at 115-120E and 50N over Northeast China and Mongolia (Figure 7). A cold front associated with this low-pressure system at 50^{o} N, 125^{o}E on April 8, 2001 lifted the dust and industrial pollutants from the lower troposphere into the middle and upper troposphere where it was then transported across the Pacific Ocean by strong zonal flow near 500mb. A comparable dust event in April 1998 occurred under similar synoptic conditions whereby a low-pressure system and frontal activity allow severe dust storms to develop over the Asian deserts and be lifted into the upper troposphere where it is transported across the Pacific Ocean to North America by strong zonal flow [*Husar et al., 2001*]. Backward trajectories also corroborate the lifting of the air mass on April 8 after it passed through the industrial regions of the Northeast Asian continent. The backward trajectory calculation for April 8 shows vertical movement of 1.5km over a 24 hour period from 2.5km to 4.0km.

The aerosol index derived from the TOMS instrument on board the Earthprobe satellite for April 8 and 14 of 2001 are shown in Plate 12a and 12b. On April 8 high

levels of UV-absorbing aerosols were observed over East Asia including dust in northern Asia and smoke from typical biomass burning regions in SE Asia during spring 2001 [*Heald et al., this issue*]. Over the next six days the TOMS data tracked the northern dust laden air masses moving across the Pacific Ocean, arriving at the west coast of North America on April 13-14 (Plate 12b). In addition, the GEOS-Chem transport model showed its highest Northeast Pacific CO level for the 2001 spring campaign on April 14th. The tagged source simulation confirms an Asian industrial source for much of this CO [*Jaeglé et al., this issue*].

Others have reported on the dust and transport aspects of this event [*Thulasiraman et al., 2002; Gong et al., 2002; Jaffe et al., 2003*]. *Thulasiraman et al.* [2002] reported on sunphotometric measurements of the dust as it passed over the North American continent, *Gong et al.* [2002] use a GCTM to model the transport of Asian dust during 2001, and *Jaffe et al.* [2003] contrasted 6 different episodes of Pacific LRT.

4.2.2 April 25, 2001 (Flight 9)

During flight 9 on April 25, 2001 a well-aged marine airmass was sampled. A comparison of flight 9 with the spring 2001 background for CO, aerosol scatter, ozone, ethane, propane and ethyne is shown in Figure 8. Mixing ratios for all species were significantly lower than the spring 2001 average with the exception of water vapor. The 0-6km mean water vapor mixing ratio (3.5ppthv) and airmass temperature (-3°C) were substantially higher compared to the spring 2001 means of 2.2ppthv and –12°C, respectively. Mixing ratios for CO and ozone averaged over 0-6km were 112ppbv and 36ppbv, well below the spring 2001 0-6km averages of 138ppbv, 45ppbv, respectively. In addition, NMHCs such as ethane and propane were observed at mixing ratios of 710 and 86pptv, 43 and 69 percent lower than mean 2001 mixing ratios of 1240 and 276pptv,

respectively. Relatively short-lived gases, including i-butane and toluene had very low mixing ratios of about 3 and 5 pptv, respectively. The ethane/propane and CO/acetylene ratios of 6.0 ± 1.5 and 0.59 ± 0.16 (per carbon), respectively, observed at 0-6km on April 25, are significantly higher than the spring 2001 ratios at 0-6km of 3.5±1.5 and 0.34±0.17 (per carbon), respectively. Such high ratios are caused by faster photochemical removal of propane and acetylene relative to ethane and CO, respectively, as well as by mixing with background air; both indicating the air was substantially aged [*McKeen et al., 1996*].

Backward trajectories (Figure 9) suggest air throughout the vertical profile (0-6km) originated in the Northwestern Pacific and was stalled in the region of the Pacific High from April 20-24. According to the trajectory calculations the air mass encountered no land contact for at least 10 days prior to sampling. Higher temperatures and greater water vapor are consistent with a lower latitude influence observed below 4km. Sea level pressure for this period shows the Pacific High split into two centers, one at 175W and 33N and the other at 140W and 33N. Trajectories suggest the airmass moved between these centers and the Aleutian Low and was stalled in the region of the Pacific high before transport to the Northwest United States. Above 4 km a layer of drier air contained mixing ratios of CO, O_3, and NMHCs that were closer to the spring 2001 averages.

4.2.3 May 6, 2001 (Flight 12)

On flight 12 chemical, meteorological data, and backward trajectories suggest that both a photochemically aged airmass and one containing fresher emissions transported from the Eurasian continent were encountered. Vertical profiles shown in Figure 10 for σ_{sg}, CO and ozone show a significant enhancement between 2-3km, compared to the spring 2001 mean. Maximums for ozone and aerosol scatter were observed at 2.9km and

2.3 km, respectively. Water vapor shows a minimum of 0.29 ppthv, coincident with an increase in aerosol scatter. Elevated mixing ratios of CO and O_3 correspond to backward trajectories originating over the Eurasian region. In addition, the ethane/propane ratio increases substantially with altitude from 3.48 at 3km to 6.73 ± 1.60 at 3.5-6km (on a per carbon basis). The ratios at 3.5-6km are similar to ratios of well-processed air observed during the April 25 flight, while the ratio at 3km are more representative of aged Eurasian outflow.

During this flight ozone is strongly correlated with both aerosol scatter ($r^2 = 0.74$) and CO ($r^2 = 0.92$). These correlations suggest photochemical production of ozone from precursors emitted from Eurasian sources. The magnitude of r^2 gives a rough measure of the fraction of the variance in a dependent variable that can be captured by a linear dependence upon an independent variable [*Draper and Smith, 1998*]. So during flight 12 on May 6, 2001 three quarters of the variance in ozone can be captured by a linear dependence upon aerosol scatter and more than 90 percent of the variance in ozone can be captured by a linear dependence upon CO.

Backward trajectories (Figure 11) for May 6, 2001 suggest a vertical split in flow patterns with aged North Pacific boundary layer air above ~3km and Eurasian LRT air below. According to the trajectory calculations, air above ~3km originated in the central North Pacific and cycled from about April 28 to May 5 in the marine boundary layer around the Pacific High, while air observed below ~3km is a combination of arctic and Eurasian air.

The GEOS-Chem chemical transport model simulation for May 6, 2001 also suggests aged emissions above 3km and Eurasian emissions below [*Jaeglé et al., this issue*]. According to the model, elevated mixing ratios observed at ~3km and below were

dominated by Asian emissions. The model's elevated mixing ratio for Asian CO at ~3km is consistent with our observation of CO at 3km. Observations of aerosol scatter and ozone also show peaks at 2-3km and ~3km, respectively, and are attributed to LRT from Eurasia.

5. SUMMARY AND CONCLUSION

In this paper we described the results of airborne measurements of CO, O_3, NMHC and aerosol scatter made during the 2001 PHOBEA field campaign near the coast of Washington State. The source regions and synoptic conditions associated with these observations are examined. A number of models and satellite tools were employed to aide in planning flight days and later in the interpretation of data and source regions.

There are a number of significant differences between the 1999 and 2001 aircraft observations in terms of the mean mixing ratios and source regions. Mean springtime mixing ratio for ozone was higher in 1999, according to both the PHOBEA aircraft observations and a comparison of Trinidad Head ozonesondes.

A number of case studies were explored including the major dust and pollution event on April 14, 2001 (flight 8). This event, observed at 3.5-6km, was unique in a number of respects: (1) the highest aerosol scatter and CO observed in 2001; (2) it was the only flight with low Ångstrom exponent (0.7) indicating dominance of super micron aerosols and; (3) the only flight with a negative relationship between aerosol scatter and ozone (r = -0.30). This negative correlation is attributed to mineral dust-ozone interactions.

Positive correlations for all flights between 0-6km were observed between CO and O_3 and, with the exception of flight 8, between aerosol scatter and ozone. This

suggests that the observed CO, ozone, and aerosol scatter are associated with similar sources, most likely industrial and/or biomass burning.

This project provided the opportunity to cover the NE Pacific, collecting the largest number of whole air samples in the region of any project to date. Together with previous PHOBEA ground and aircraft observations from the springs of 1997 through 2001 these data comprise the most comprehensive database of tropospheric chemistry in the northeastern Pacific during spring.

APPENDIX: EVALUATION OF DUCHESS AEROSOL INLET PASSING EFFICIENCY DURING THE PHOBEA 2001 AIRCRAFT FLIGHTS.

As described in the Experimental section, aerosols were sampled through a rear facing stainless steel inlet with a 3/16" i.d. Air was pulled through the inlet using a small vacuum pump into the TSI 3 λ nephelometer (450, 550, 700 nm) at a volumetric flow rate of approximately 25 liters per minute. In this configuration we do not expect that larger aerosol particles will pass through the inlet. It therefore becomes important to estimate the aerosol cutoff diameter for this configuration.

One approach to doing this is using the measured Ångström (å) exponent, or wavelength dependence of scattering, since å is a strong function of the aerosol size distribution. It is defined as:

$$\text{å}(\lambda_1/\lambda_2) \equiv -\log\left(\sigma_{sp,\lambda_1}/\sigma_{sp,\lambda_2}\right)/\log(\lambda_1/\lambda_2) \quad (1)$$

For visible wavelengths, both Mie Theory calculations (Figure A1) and experimental data [*Delene and Ogren, 2001*] show that å typically ranges from ca. 3 to 1 for sub-micron particles (with strong size dependence) and is near zero for supermicron particles.

To evaluate the inlet size cut, we use observations from April 14th, 2001. On this date, aerosols from a large Asian dust episode were transported to the west coast of North America. Our vertical profiles on April 14th, showed substantial aerosol scattering between 4-6 km (Figure 5). It is reasonable to assume that the volume size distribution of this dust aerosol peaks at super-micron sizes, making this an ideal case to evaluate the aerosol inlet. For this purpose, Mie calculations were used to simulate the values of å that would be measured by the three-wavelength nephelometer for different assumed values of the inlet cut size. The dust aerosol was represented as a lognormal distribution with a volume mean geometric diameter of 4.0 μm, a geometric standard deviation of 2.0, a real refractive index of 1.5 and an imaginary refractive index of 0. (Results are not sensitive to these choices.) We used modified Mie calculations that took into account the known scattering geometry of the nephelometer [*Anderson et al., 1996*] and we compare to nephelometer measurements that have not been corrected for angular non-idealities. The Mie calculation results are shown in Figure A1 for both å(450/550) and å(550/700), denoted ABG and AGR, respectively.

Within the heaviest dust layers, the observed value of å(450/550) was 0.6 and the observed value of å(550/700) was 0.8. These values are very different from the values observed in non-dust layers of ~2.0. This reflects the prevalence of larger aerosol particles during the dust event of April 14th, 2001. Using the measured values of å in these dust layers and Figure A1, we find that the results are consistent with an aerosol inlet cut-size of 0.7 +/- 0.1 μm geometric diameter.

Jaffe et al., [2003] report on gas and aerosol measurements during 6 identified trans-Pacific long range transport events, spanning observations from 1993-2001. In all of these cases where å could be calculated, values of 2.0-2.5 were found, except for April

14th, 2001 (flight 8). An important conclusion from this is that for April 14th our inlet cut-size of 0.7+/-0.1 μm must be excluding a large fraction of the aerosol mass. For the other cases, the portion of the excluded mass is not known, but the results herein indicate that the sub-micron aerosol mass is effectively sampled by our inlet.

ACKNOWLEDGMENTS

We would like to thank Lyatt Jaeglé and Daniel Jacob for their comments, suggestions and work with the GEOS-Chem model, Richard Gammon and Roy Farrow for their work on the RGA, Peter Hess for his assistance with the PV interpretation, James Dennison for preparing figure 1, Robert Kotchenruther and Northway Aviation for help with the aircraft and instrumentation, and Tai Chen for his assistance with ACE-Asia NMHC data. This work was supported by NSF grant ATM-0089929, the Canadian Foundation for Climate and Atmospheric Sciences, and a Department of Energy Graduate Research Environmental Fellowship. The careful reviews by two anonymous reviewers are gratefully acknowledged.

REFERENCES

Akimoto, H., and H. Narita, Distributions of SO_2, NOx, and CO_2 emissions from fuel combustion and industrial activities with 1x1 resolution *Atmos. Environm., 28,* 213-225, 1994.

Anderson, T. L., D. S. Covert, S. Marshall, M. L. Laucks, R. J. Charlson, A. P. Waggoner, J. A. Ogren, R. Caldow, R. Holm, F. Quant, G. Sem, A. Wiedensohler, N. A. Ahlquist, and T. S. Bates, Performance characteristics of a high-sensitivity, three-wavelength, total scatter/backscatter nephelometer, *J. Atmos. Oceanic Technol., 13*, 967-986, 1996.

Andreae, M. O., H. Berresheim, T. W. Andreae, Vertical distribution of dimethyl sulfide,

sulfur dioxide, aerosol ions and radon over the northeast pacific ocean, *J. Atmos. Chem., 6,* 149-173, 1988.

Bailey, R., L. A. Barrie, C. J. Halsall, P. Fellin, and D. C. Muir, Atmospheric organochlorine pestisides in the western Canadian Arctic: Evidence of Trans-Pacific Transport, *J. Geophys. Res., 105,* 11,805, 11,811, 2000.

Berntsen, T. J., S. Karlsdottir, D. A. Jaffe, Influence of Asian emissions on the composition of air reaching the North Western United States, *Geophys. Res. Lett.*, *26*, 2171-2174, 1999.

Bey I., D. J. Jacob, R. M. Yantosca, J. A. Logan, B. Field, A. M. Fiore, Q. Li, H. Liu, L. J. Mickley, and M. Schultz, Global modeling of tropospheric chemistry with assimilated meteorology: Model description and evaluation*, J. Geophys. Res.*, *106*, 23,073-23,096, 2001.

Bognar, J. A., and J. W. Birks, Miniaturized Ultraviolate Ozonesonde for Atmospheric Measurements, *Anal. Chem., 68,* 3059-3062, 1996.

Bolton, D., The computation of Equivalent Potential Temperature, *Monthly Weather Review, 108,* 1046-1053, 1980.

Delene, D. J., and J. A. Ogren, Variability of aerosol optical properties at four North American surface monitoring sites, *J. Atmos. Sci., 59*, 1135-1150, 2001.

Dentener, F. J., G. R. Carmichael, Y. Zang, J. Lelieveld, and P. Crutzen, Role of mineral aerosol as a reactive surface in the global troposphere, *J. Geophys. Res., 101*, D17, 22,869-22,889, 1996.

Dickerson, R. R., S. Kondragunta, G. Stenchikov, K .L. Civerolo, B. G. Doddridge, and G. N. Holben, The impact of aerosols on solar ultraviolet radiation and photochemical smog, *Science, 278*, 827-830, 1997.

Doskey, P. V., and H. M. Bialk, Automated sampler for the measurement of non-methane organic compounds, *Environ. Sci. Technol., 35*, 591-594, 2001.

Doskey, P. V., and J. S. Gaffney, Non-methane hydrocarbons in the arctic atmosphere at Barrow, Alaska, *Geophys. Res. Lett., 19,* 4, 381-384, 1992.

Draper, N. R., and H. Smith, Applied Regression Analysis, 3rd ed., John Wiley, New York, 1998.

Draxler, R. R., and G. D. Hess, An overview of the HYSPLIT_4 modeling system for trajectories, dispersion and deposition, *Aust. Met. Mag., 47*, 295-308, 1998.

Draxler, R. R., and G. D. Hess, Description of the HYSPLIT_4 modeling system, *NOAA Technical Memorandum ERL ARL-224*, 24, 1997.

Duncan, B., R. Martin, A. Staudt, R. Yevich and J. Logan, Interannual and Seasonal Variability of Biomass Burning Emissions Constrained by Satellite Observations, submitted to *J. Geophys. Res*., March 2002.

Fiore, A. M., D. J. Jacob, I. Bey, R. M. Yantosca, B. D. Field, A. C. Fusco, and J. G. Wilkinson, Background ozone over the United States in summer: Origin, trend, and contribution to pollution episodes, *J. Geophys. Res., 107*, D15, n4275, 2002.

Galbally, I. E., and C. R. Roy, Destruction of ozone at the earth's surface, *Q. J. R. Meteorol. Soc., 106*, 559-620, 1980.

Gong, S. L., X. Y. Zhang, T. L. Zhao, I. G. McKendry, D. A. Jaffe, and N. M. Lu, Characterization of soil dust aerosol in China and its transport/distribution during 2001 ACE-Asia: 2. Model Simulation and Validation, *J. Geophys. Res.,* submitted August 2002.

Gregory, G. L., A. S. Bachmeier, D. R. Blake, B. G. Heikes, D. C. Thornton, A. R. Bandy, J.D. Bradshaw, and Y. Kondo, Chemical signatures of Pacific marine air:

Mixed layer and free troposphere as measured during PEM-West A, *J. Geophys. Res., 101,* D1, 1727-1742, 1996.

Heald, C. L., D. J. Jacob, P. I. Palmer, M. J. Evans, G. W. Sachse, H. B. Singh and D. R. Blake, Biomass burning emission inventory with daily resolution: application to aircraft observations of Asian outflow, *J. Geophys. Res.,* this issue.

Huebert, B., T. Bates, P. Russell, J. Seinfeld, M. Wang, M. Uematsu, and Y. J. Kim, An overview of ACE-Asia: strategies for quantifying the relationships between Asian aerosols and their climatic impacts., submitted to *J. Geophys. Res.*, 2002.

Holton, J. R., P. H. Haynes, M. E. McIntyre, A. R. Douglass, R. B. Rood and L. Pfister, Stratosphere-troposphere exchange, *Reviews of Geophysics, 33,* 403-439, 1995.

Hoskins, B. J., M. E. McIntyre and A. W. Robertson, On the use and significance of isentropic potential vorticity maps, *Quart. J. Roy. Meteorol. Soc., 111*, 877-946, 1985.

Husar, R. B., D. M. Tratt, B. A.Schichtel, S. R. Falke, F. Li, D. Jaffe, S. Gassó, T. Gill, N. S. Laulainen, F. Lu, M. C. Reheis, Y. Chun, D. Westphal, B. N. Holben, C. Gueymard, I. McKendry, N. Kuring, G. C. Feldman, C. McClain, R. J. Frouin, J. Merrill, D. DuBois, F. Vignola, T. Murayama, S. Nickovic, W. E. Wilson, K. Sassen, N. Sugimoto, W. C. Malm, Asian dust events of April 1998, *J. Geophys. Res., 106,* 18,317-18,330, 2001.

IPCC, (2001a). Climate Change 2001: Impacts, Adaptation and Vulnerability. Cambridge University Press. Cambridge.

Jacob, D .J., J. H. Crawford, J. M. Kleb, V. E. Connors, R. J Bendura, J. L. Raper, G. W.

Sachse, J. C. Gille, L. Emmons, The Transport and Chemical Evolution over the Pacific (TRACE-P) Mission: Design, Execution, and Overview of First Results, *J. Geophys. Res.,* this issue.

Jacob, D. J., J. A. Logan, P. P. Murti, Effect of rising Asian emissions on surface ozone in the US, *Geophys. Res. Lett., 26,* 2175-2178, 1999.

Jaeglé, L., D. A. Jaffe, H. U. Price, P. Weiss-Penzias, P. I. Palmer, M. J. Evans, D. J. Jacob, and I. Bey, Sources and Budgets for CO and O_3 in the Northeastern Pacific during the spring of 2001: Results from the PHOBEA-II Experiment, *J. Geophys. Res.*, this issue.

Jaffe, D.A., I. McKendry, T. Anderson, H.U. Price, Six episodes of Trans-Pacific Transport of Air Pollutants, *Atmos. Environm., 37,* 391-404, 2003.

Jaffe, D. A., T. Anderson, D. Covert, B. Trost, J. Danielson, W. Simpson, D. Blake, J. Harris, D. Streets, Observations of ozone and related species in the northeast Pacific during the PHOBEA campaigns 1. Ground-based observations at Cheeka Peak, *J. Geophys. Res., 106,* D7, 7449-7461, 2001.

Jaffe, D. A., T. Anderson, D. Covert, R. Kotchenruther, B. Trost, J. Danielson, W. Simpson, T. Berntsen, S. Karlsdottir, D. Blake, J. Harris, G. Carmichael, I. Uno, Transport of Asian air pollution to North America, *Geophys. Res. Lett., 26,* 711-714, 1999.

Jaffe, D. A., T. K. Berntsen, I. S. A. Isaksen, A global 3-D chemical transport model 2. Nitrogen oxides and NMHC results, *J. Geophys. Res.*, *102*, 21281-21296, 1997.

Kato, S., P. Pochanart, and Y. Kajii, Measurements of ozone and nonmethane

hydrocarbons at Chichi-jima island, a remote island in the western Pacific: long range transport of polluted air from the Pacific rim region, *Atmos. Environm., 35,* 6021-6029, 2001.

Kato, N., and H. Akimoto, Anthropogenic emissions of SO2 and NOx in Asia: Emission inventories, *Atmos. Environm., 26,* 2997-3017, 1992.

Kotchenruther, R. A., D. A. Jaffe, H. J. Beine, T. L. Anderson, J. W. Bottenheim, J. M. Harris, D. R. Blake, R. Schmitt, Observations of ozone and related species in the northeast Pacific during the PHOBEA campaigns 2. Airborne observations, J. *Geophys. Res., 106*, D7, 7463-7483, 2001.

McKeen, S. A., S. C. Liu, E. Y. Hsie, X. Lin, J. D. Bradshaw, S. Smyth, G.L. Gregory, D. R. Blake, Hydrocarbon ratios during PEM-WEST A: A model perspective, *J. Geophys. Res., 101,* D1, 2087-2109, 1996.

Parrish, D. D., C. J. Hahn, E. J. Williams, R. B. Norton, F. C. Fehsenfeld, H. B. Singh, J. D. Shetter, B. W. Gandrud, B. A. Ridley, Indication of photochemical histories of pacific air masses from measurements of atmospheric trace species at Point Arena, California, *J. Geophys. Res., 97*, 15,883-15,901, 1992.

Phandis, M. J., and G. R. Carmichael, Transport and distribution of primary and secondary nonmethane volatile organic compounds in east Asia under continental outflow conditions, *J. Geophys. Res., 105*, D17, 22,311-22,336, 2000.

Ridley, B. A. et al., Aircraft measurements made during the spring maximum of ozone over Hawaii: Peroxides, CO, O_3, Noy, condensation nuclei, selected hydrocarbons, halocarbons, and alkyl nitrates between 0.5 and 9 km altitude, *J. Geophys. Res., 102,* 18,935-18,961, 1997.

Snow, J., J. B. Dennison, D. A. Jaffe, H. U. Price, J. K. Vaughan, B. Lamb, I. G.

McKendry, Aircraft Measurements of Air Quality in Puget Sound: Summer 2001, submitted to *Atmos. Environm., September 2002*.

Staudt, A. C., D. J. Jacob, J. A. Logan, D. Bachiochi, T. N. Krishnamurti, and G. W. Sachse, Continental sources, transoceanic transport, and interhemispheric exchange of carbon monoxide over the Pacific, *J. Geophys. Res., 106*, 32,571-32,590, 2001.

Stohl, A., 1-year Lagrangian "climatology" of airstreams in the Northern Hemisphere troposphere and lowermost stratosphere, *J. Geophys. Res., 106,* 7263-7279, 2001.

Streets, D. G., and S. T. Waldhoff, Present and future emissions of air pollutants in China,SO2, NOx, and CO, *Atmos. Environm., 34*, 364-374, 2000.

Talbot, R.W., et al., Chemical characteristics of continental outflow from Asia to the troposphere over the western Pacific Ocean during February-March 1994: Results from PEM-West B, *J. Geophys. Res., 102,* 28,255-28,274, 1997.

Thulasiraman S., N. T. O'Neill, A. Royer, B. N. Holben, D. Westphal, L. J. B. McArthur, Sunphotometric observations of the 2001 Asian dust storm over Canada and the U.S., *Geophysical Research Letters, 29,* 8, 2002.

van Aardenne, J. A., G. A. Carmichael, H. Levy, D. Streets, L. Hordijk, Anthropogenic NOx emissions in Asia in the period 1990-2020, *Atmos. Environm*., 33, 633-646, 1999.

FIGURE CAPTIONS:

Figure 1. Schematic diagram of Duchess aircraft interior.

Figure 2. Aerosol scatter (550nm) versus CO at 0-6km.

Figure 3. One minute averaged ozone versus aerosol scatter (550nm) at 0-6km.

Figure 4. Trinidad Head ozonesonde comparison.

Figure 5. Spring 2001 marine mean ± 1σ and 1-second data from flight 8 on April 14, 2001. NMHCs and CO are from 5-minute canister samples.

Figure 6. NOAA HYSPLIT READY 10day backward trajectory arriving on 14 April 2001 at 4.9-6 km.

Figure 7. Mean sea level pressure on 8 April 2001.

Figure 8. Spring 2001 marine mean ± 1σ and second data from flight 9 on April 25, 2001. NMHCs and CO are from 5-minute canister samples.

Figure 9. NOAA HYSPLIT READY 10day backward trajectory arriving on April 25, 2001at 0-6km.

Figure 10. Spring 2001 marine mean ± 1σ and second data from flight 12 on May 6, 2001. NMHCs and

CO are from 5-minute canister samples.

Figure 11. NOAA HYSPLIT READY 10day backward trajectory arriving May 6, 2001 at 1.5-3.5 km.

Plate 12a,b. TOMS satellite image of aerosol index on (a) 8 April 2001 and (b) 14 April 2001.

Figure A1. Ångstrom Exponent.

Table 1. Flight information. Flight times are in Greenwich Mean Time and represent sampling start times.

Flight	Flight Date	Flight Time	General air mass types encountered
1	March 29	4:30	North Pacific and Eurasian Arctic
2	March 31	3:40	North Pacific <4km, Eurasia >4km
3	April 1	22:40	North Pacific and Eurasia
4	April 5	3:00	North American influence <3.5km (local), North Pacific >3.5km
5	April 8	17:30	North American influence (western continental US)
6	April 9	21:15	North Pacific and Eurasia
7	April 11	18:00	North American influence (Canada)
8	April 14	1:00	Asian LRT event with enhanced CO, NMHC, aerosol scatter >3.5km
9	April 25	18:30	North Pacific (stalled in region of Pacific High, well processed)
10	April 27	23:50	North Pacific (Eurasia >1km, well processed < 1km)
11	May 1	18:00	North Pacific (stalled in region of Aleutian Low)
12	May 6	18:00	Eurasian LRT <3km, North Pacific well processed >3km

Table 2. Aircraft Data From PHOBEA 2001 Aircraft Experiment, segregated by Altitude. Mixing ratios are presented in parts per trillion by volume unless otherwise noted and N represents the number of individual flight segments at that altitude contributing to the reported average. North American continental influenced flight legs (flights 4 (<3.5km), 5, and 7) are not included in Marine data column. σ_{sg} is aerosol scatter at the green wavelength (550nm), relative to STP.

	O_3, ppbv		σ_{sg}, Mm^{-1}		H_2O		Temp, C		CO, ppbv		Ethane		Propane	
	All	Marine	All	Marine	All	Marine	All	Marine	All	Marine	All	Marine	All	Marine
0-1.5km														
Average	43	43	2.39	2.68	4.8	5.3	1.2	1.6	153	151	1379	1300	309	274
s.d. (1sd)	6	7	1.08	1.04	2.2	2.2	4.3	4.9	16	16	284	258	103	78
median	44	44	2.30	2.35	5.0	5.2	0.8	-0.5	159	158	1401	1385	304	295
minimum	29	29	1.06	1.45	2.1	3.0	-2.2	-2.2	121	121	924	924	163	163
maximum	52	52	4.13	4.13	9.2	9.2	11.8	11.8	166	166	1692	1508	448	343
N	9	7	9	7	9	7	9	7	7	6	5	4	5	4
1.5-2.5 km														
Average	45	47	4.74	5.33	2.6	2.8	-5.5	-4.9	144	143	1515	1366	419	328
s.d. (1sd)	11	12	6.46	7.10	1.6	1.7	5.0	5.6	20	23	394	344	200	143
median	43	45	2.69	3.08	2.2	3.1	-6.2	-6.3	148	149	1478	1430	419	343
minimum	30	30	0.19	0.25	0.2	0.2	-10.5	-10.5	96	96	651	651	91	91
maximum	72	72	20.98	20.98	4.6	4.6	8.1	8.1	167	167	2047	1843	720	550
N	12	9	12	9	12	9	12	9	11	8	11	8	11	8
2.5-3.5 km														
Average	45	46	3.25	3.45	1.7	1.9	-10.5	-9.5	139	136	1354	1230	364	290
s.d. (1sd)	9	10	3.58	4.02	1.3	1.4	5.7	5.9	15	14	332	268	189	125
median	46	47	2.50	1.84	1.6	1.9	-9.3	-9.2	139	138	1317	1303	332	320
minimum	30	30	0.22	0.33	0.3	0.3	-19.2	-19.2	114	114	639	639	78	78
maximum	61	61	12.88	12.88	4.1	4.1	0.0	0.0	164	156	1949	1486	802	470
N	12	9	12	9	12	9	12	9	12	9	12	9	12	9
3.5-4.5 km														
Average	44	43	4.19	3.76	1.3	1.5	-15.8	-14.6	135	133	1240	1197	282	262
s.d. (1sd)	9	10	4.75	4.38	1.1	1.1	6.9	6.8	23	24	325	336	132	129
median	47	48	2.49	2.49	0.7	1.1	-15.8	-13.4	140	140	1341	1243	289	282
minimum	24	24	0.28	0.28	0.2	0.3	-26.9	-26.9	91	91	586	586	50	50
maximum	54	54	14.87	14.87	3.1	3.1	-4.4	-4.4	174	174	1600	1600	476	427
N	12	10	12	10	12	10	12	10	12	10	12	10	12	10
4.5-5.5 km														
Average	44	45	4.77	5.37	0.8	0.9	-22.2	-20.9	138	136	1225	1224	269	272
s.d. (1sd)	10	10	7.53	8.16	0.7	0.7	6.2	5.7	25	27	361	385	142	152
median	46	46	2.60	2.60	0.5	0.6	-21.6	-19.6	145	128	1350	1317	271	269
minimum	22	22	0.54	0.54	0.1	0.2	-32.5	-30.3	103	103	596	596	70	70
maximum	56	56	28.25	28.25	2.2	2.2	-13.5	-13.5	184	184	1699	1699	530	530
N	12	10	12	10	12	10	12	10	12	10	12	10	12	10
5.5-6 km														
Average	45	46	6.00	7.05	0.6	0.7	-26.9	-25.6	133	130	1173	1126	250	234
s.d. (1sd)	9	10	11.40	12.31	0.6	0.6	6.6	6.2	20	21	306	299	125	125
median	45	45	1.60	2.67	0.4	0.4	-26.0	-25.6	130	126	1153	1100	223	209
minimum	29	29	0.43	0.66	0.1	0.1	-37.6	-33.6	106	106	672	672	52	52
maximum	61	61	41.30	41.30	1.8	1.8	-16.2	-16.2	173	173	1617	1558	436	436
N	12	10	12	10	12	10	12	10	11	9	11	9	11	9

Table 2. (continued)

	Ethyne		CH_3Cl		n-butane		i-butane		i-pentane		pentane		benzene	
	All	Marine	All	Marine	All	Marine	All	Marine	All	Marine	All	Marine	All	Marine
0-1.5km														
Average	262	226	622	651	51	32	36	28	22	19	6	3	75	67
s.d. (1sd)	103	75	112	105	44	16	25	21	10	9	8	1	32	30
median	218	211	601	620	34	33	31	26	24	20	3	2	66	64
minimum	152	152	504	564	12	12	5	5	9	9	1	1	35	35
maximum	407	329	801	801	126	51	66	55	33	27	18	4	108	107
N flights	5	4	5	4	5	4	5	4	4	3	4	3	5	4
1.5-2.5 km														
Average	310	294	566	574	136	116	57	41	26	21	19	18	90	88
s.d. (1sd)	114	132	26	25	76	76	37	28	16	13	9	10	45	54
median	336	307	568	570	122	105	63	33	24	19	21	18	84	76
minimum	68	68	522	542	23	23	5	5	9	9	6	6	26	26
maximum	441	441	623	623	233	211	120	86	46	38	30	30	209	209
N flights	11	8	11	8	11	8	11	8	5	4	5	4	11	8
2.5-3.5 km														
Average	245	223	572	570	105	91	43	30	26	22	10	7	63	56
s.d. (1sd)	81	76	19	16	64	65	32	21	14	11	9	8	26	25
median	253	238	572	569	101	73	33	28	28	24	6	6	66	56
minimum	82	82	539	539	5	5	4	4	4	4	0	0	23	23
maximum	389	349	606	593	198	195	119	71	46	33	22	20	105	105
N flights	12	9	12	9	12	9	12	9	6	5	6	5	12	9
3.5-4.5 km														
Average	233	224	566	567	81	78	33	30	20	15	6	3	57	61
s.d. (1sd)	104	108	20	22	61	64	22	21	13	6	9	2	31	32
median	228	228	565	564	88	50	29	26	17	12	3	3	56	58
minimum	58	58	545	545	3	3	3	3	9	9	1	1	15	15
maximum	398	398	612	612	171	171	69	62	43	22	24	5	125	125
N flights	12	10	12	10	12	10	12	10	6	5	6	5	12	10
4.5-5.5 km														
Average	233	227	582	583	67	72	33	35	23	26	11	12	54	58
s.d. (1sd)	98	100	22	24	62	66	34	37	13	12	10	11	35	36
median	227	227	574	574	47	47	27	26	19	23	6	7	58	61
minimum	69	69	552	552	7	7	2	2	5	13	2	2	12	12
maximum	422	422	625	625	184	184	119	119	43	43	28	28	135	135
N flights	12	10	12	10	12	10	12	10	7	6	7	6	12	10
5.5-6 km														
Average	228	222	586	591	97	107	25	24	15	17	9	10	41	43
s.d. (1sd)	109	114	28	27	91	98	22	24	8	8	7	7	18	19
median	220	220	582	592	65	65	19	18	16	16	6	10	44	52
minimum	63	63	545	551	8	8	2	2	8	8	1	1	7	7
maximum	460	460	624	624	265	265	76	76	27	27	17	17	63	63
N flights	11	9	11	9	11	9	11	9	5	4	5	4	11	9

Table 3. Linear Correlation Matrix (*r* Values) for various species.[a]

	σ_{sg}	ozone	H_2O	ethane	propane	propene	ethyne	CH_3Cl	n-butane	i-butane	n-pentane	i-pentane	benzene	CO
σ_{sg}	1.00													
ozone	0.19	1.00												
H_2O	-0.24	-0.45	1.00											
ethane	0.34	0.43	-0.27	1.00										
propane	0.38	0.35	-0.32	**0.95**	1.00									
propene	0.42	0.12	-0.17	0.39	0.42	1.00								
ethyne	0.54	0.45	-0.33	**0.89**	**0.92**	0.50	1.00							
CH_3Cl	0.04	0.06	0.30	0.07	0.09	-0.06	0.08	1.00						
n-butane	0.43	0.24	-0.38	**0.73**	**0.80**	0.51	**0.82**	0.09	1.00					
i-butane	0.35	0.30	-0.33	**0.75**	**0.84**	0.32	**0.80**	0.22	**0.74**	1.00				
n-pentane	0.39	0.00	-0.21	0.20	0.34	0.69	0.34	-0.14	0.56	0.46	1.00			
i-pentane	0.36	-0.05	-0.04	-0.02	0.12	0.40	0.15	0.17	0.26	0.30	0.54	1.00		
benzene	0.27	0.16	-0.14	**0.77**	**0.78**	0.50	**0.81**	0.02	0.63	**0.70**	0.08	0.26	1.00	
CO	0.53	0.33	-0.16	**0.79**	**0.76**	0.43	**0.81**	0.00	0.51	0.60	0.06	0.15	0.66	1.00

[a]R values in bold have an absolute value greater than or equal to 0.70. The linear correlations for σ_{sg}, ozone and H_2O are determined from 1minute averages and NMHCs and CO from 5-minute canister samples. Aerosol scatter (σ_{sg}) is relative to STP.

Table 4. Comparison of 1999 and 2001 PHOBEA aircraft observations excluding event flights[b].

Compound	Mean ± 1σ 0-6.0km				Mean ± 1σ 0-3.5km				Mean ± 1σ 3.5-6.0km			
	1999	2001	Change	*P* value	1999	2001	Change	*P* value	1999	2001	Change	*P* value
σ_{sg}, Mm^{-1}	3.8±4.7	3.4±3.8	0	0.70	2.6±3.0	4.1±5.2	-	0.92	5.8±6.1	2.9±2.1	+	0.99
Ozone	56±13	45±10	+	>0.99	52±12	45±11	+	0.98	65±12	44±10	+	>0.99
CO	132±25	133±19	0	0.61	131±23	140±18	-	0.91	133±29	128±18	+	0.76
Acetylene	354±187	221±89	+	>0.99	342±192	240±97	+	0.97	366±187	201±80	+	>0.99
Ethane	1481±515	1217±303	+	>0.99	1476±542	1268±275	+	0.92	1486±507	1135±315	+	>0.99
Propane	303±221	271±117	0	0.78	240±252	297±113	0	0.56	308±194	233±117	+	0.94
Butane	73±63	79±65	0	0.66	73±73	80±65	0	0.62	73±54	71±65	0	0.54
i-Butane	41±40	31±23	+	0.9	40±44	31±21	0	0.77	41±37	25±25	+	0.94
Pentane	12±17	8±10	+	0.89	8±10	10±10	0	0.68	15±20	7±9	+	0.96
i-Pentane	17±12	20±8	0	0.75	10±7	21±9	-	>0.99	25±15	19±7	+	0.83
CH_3Cl	583±32	582±42	0	0.53	577±29	589±57	0	0.77	589±34	580±27	+	0.83

[b]Flights excluded are April 14, 2001 (Asian dust/pollution), April 5 (<3.5km), 8 & 11, 2001, and April 9 & 28, 1999 (North American influence) and April 3, 1999 (stratospheric influence) . Full statistical analysis of data from 1999 is available in Kotchenruther et al., 2001.

Table 5. Comparison of long range transported pollution dust event observed during flight 8 on April 14, 2001 to the PHOBEA 2001background data at 3.5-6km. Mean mixing ratios are in parts per trillion by volume unless otherwise noted.

[a] Background data listed here are marine data from Table 2, but without dust event observations from April 14, 2001.

Compound	14 April 2001	Background[a]	% Enhancement
Ozone, ppbv	46	44	5
σ_{sg}, Mm^{-1}	28.30	3.01	840
H_2O, ppthv	0.28	1.11	-75
Temp, C	-22	-20	9
CO, ppbv	177	128	38
Ethane	1613	1133	42
Ethene	137	66	108
Propane	462	232	99
Propene	70	24	192
Ethyne	427	200	113
CH_3Cl	578	580	0
n-butane	203	72	181
i-butane	69	25	178
i-propane	36	19	88
Pentane	28	7	299
Benzene	108	48	124
Toluene	7	2	230

Figure 1. Schematic diagram of Duchess aircraft interior

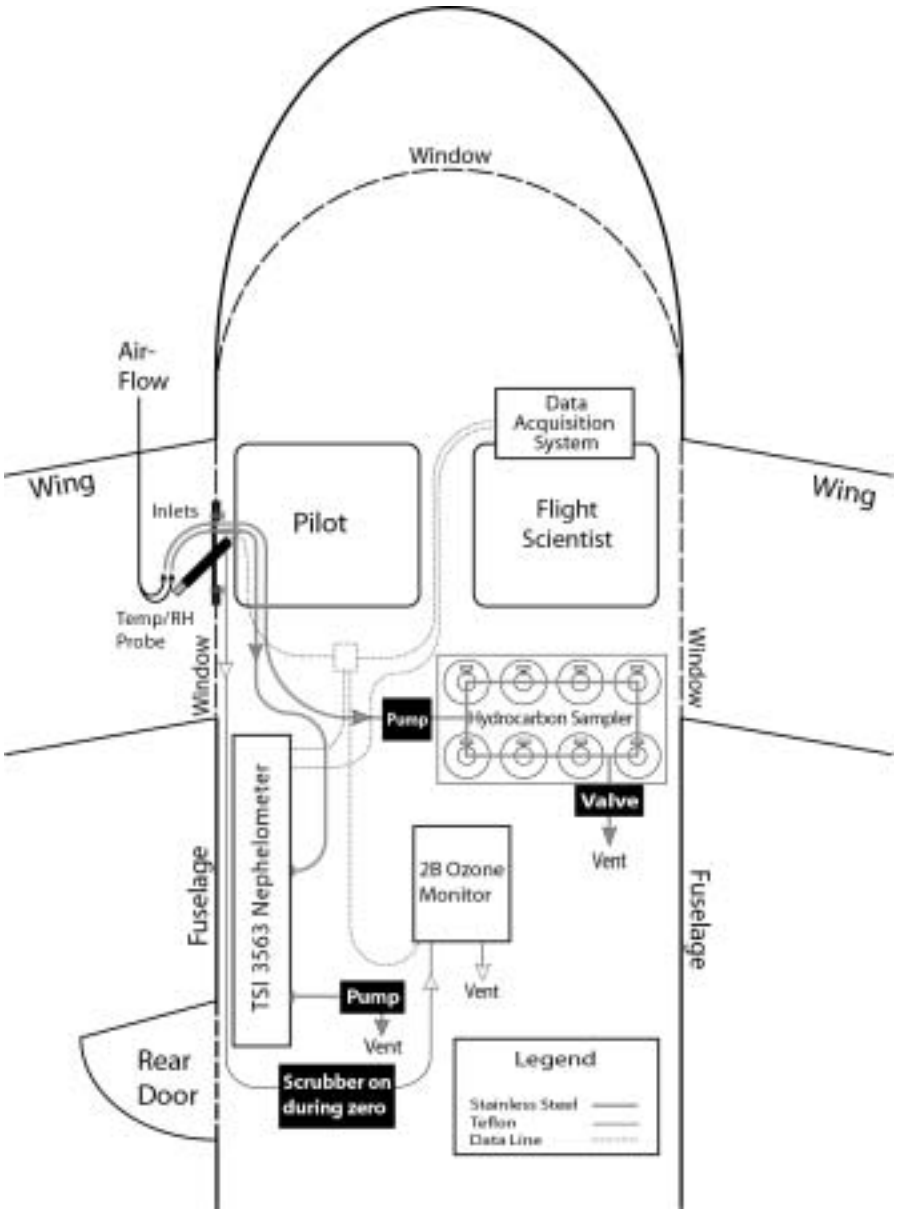

Figure 2. Aerosol scatter versus CO at 0-6km.

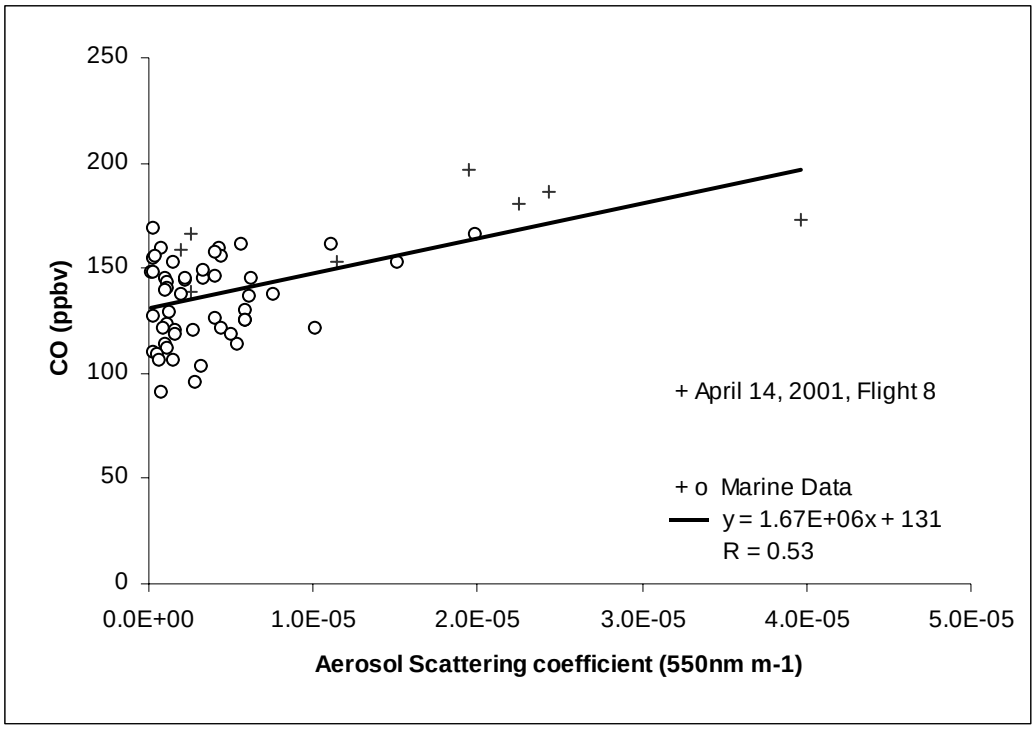

Figure 3. One minute averaged ozone versus aerosol scatter (550nm) at 0-6km.

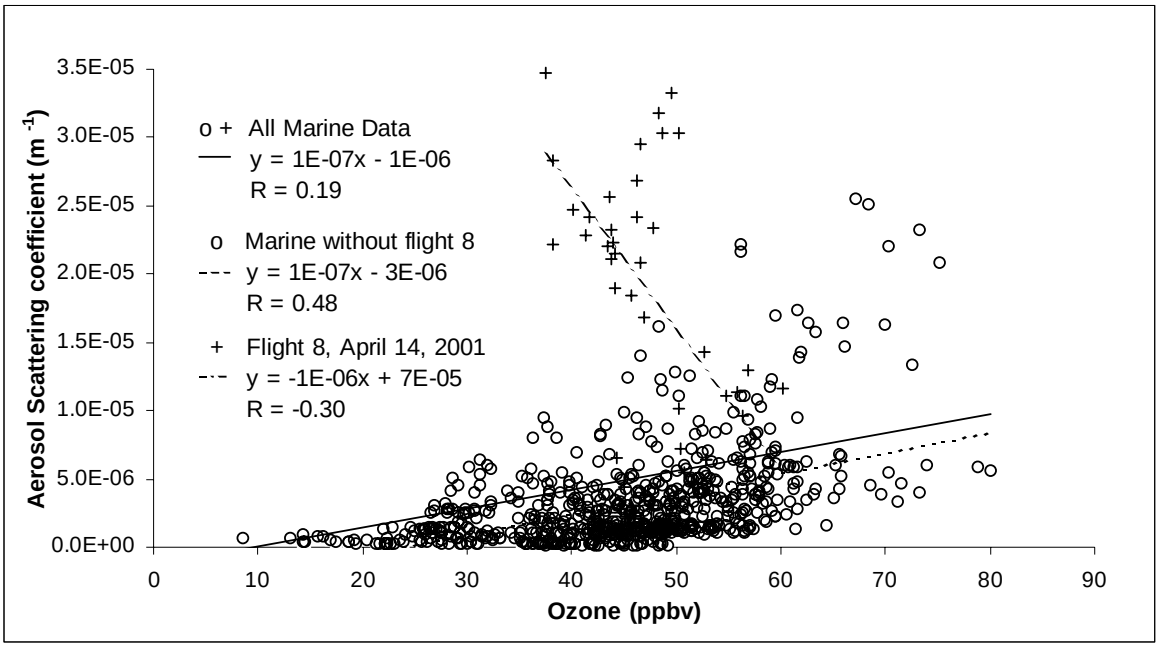

Figure 4. Trinidad Head ozonesonde comparison

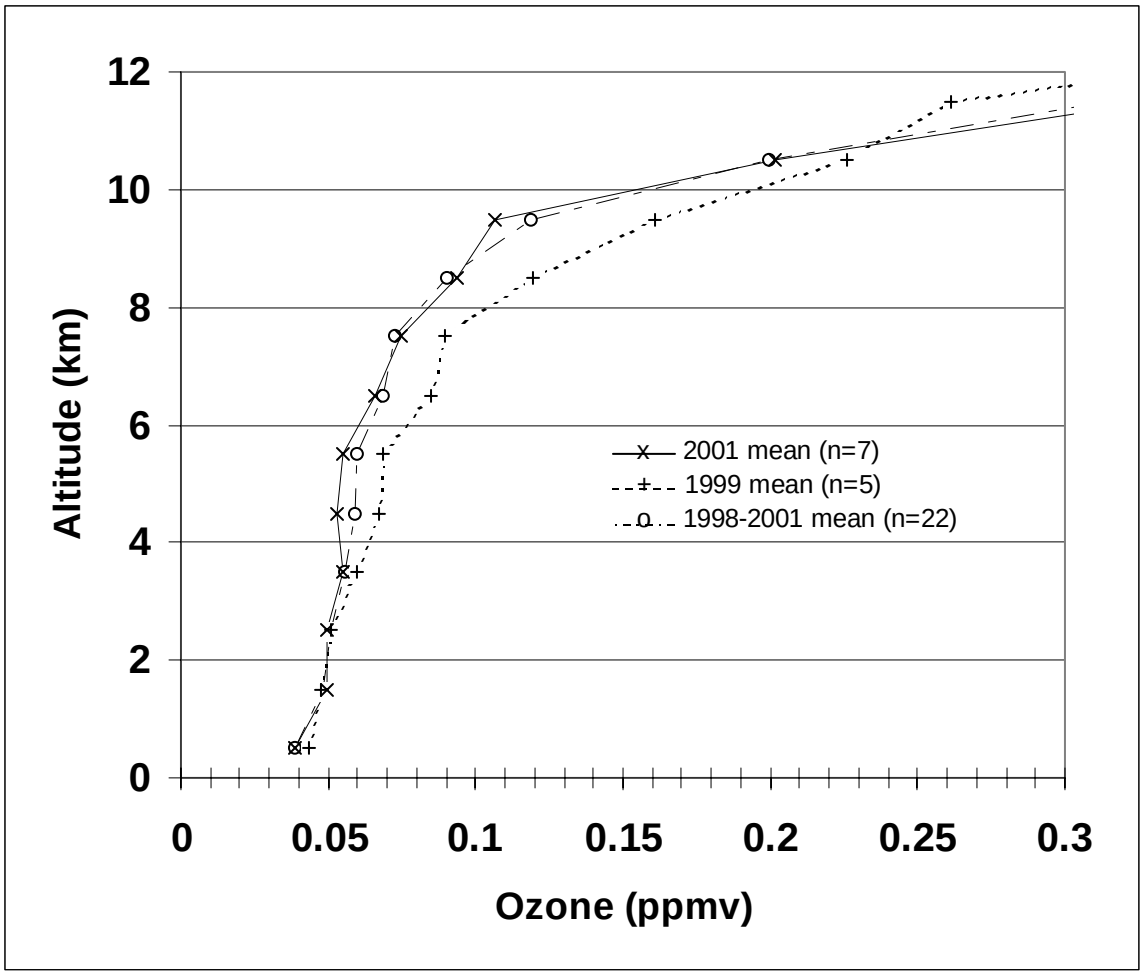

Figure 5. Spring 2001 marine mean ± 1σ and 1-second data from flight 8 on April 14, 2001. NMHCs and CO are from 5-minute canister samples.

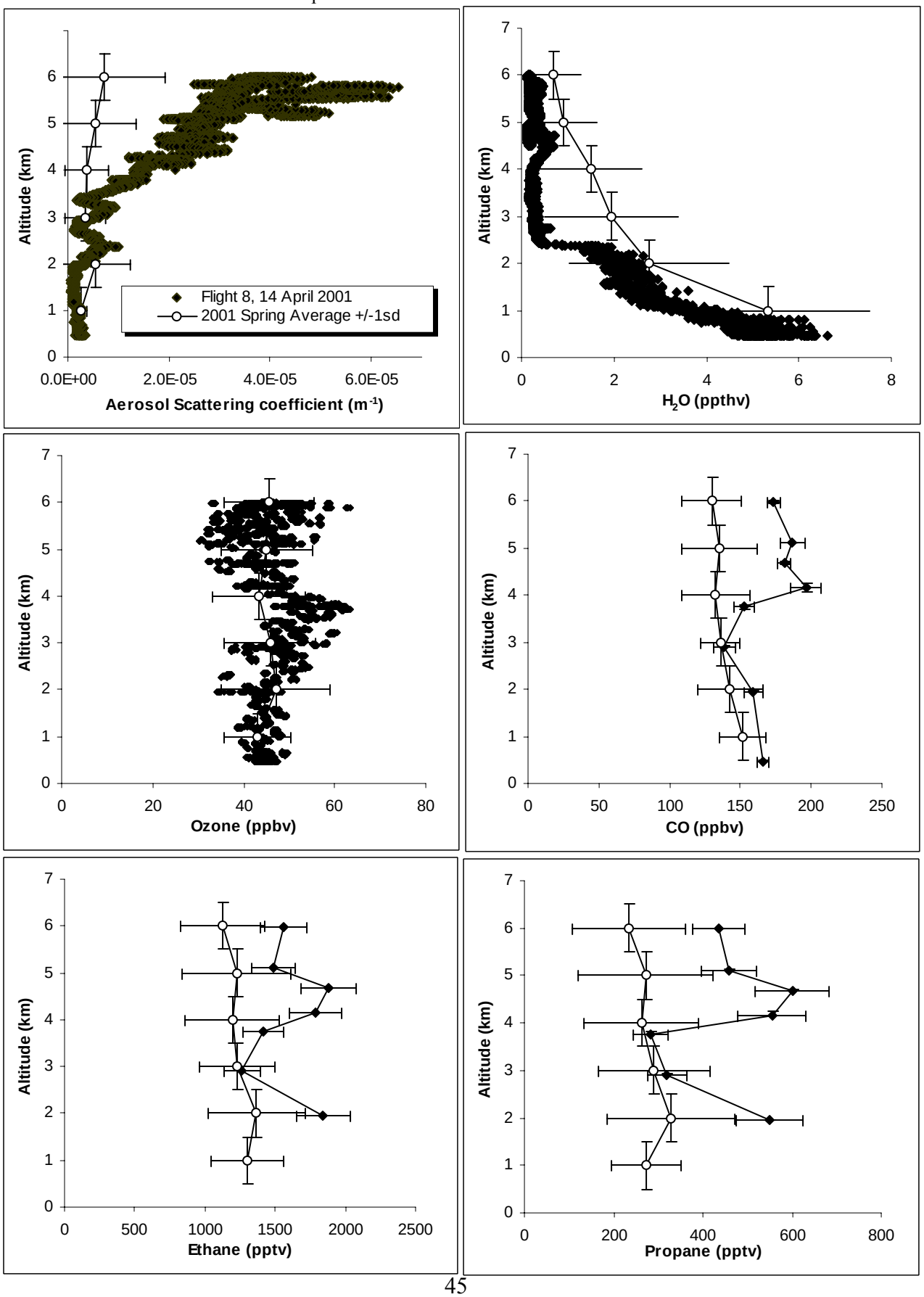

Figure 6. NOAA HYSPLIT READY 10day backward trajectory arriving on 14 April 2001 at 4.9-6 km.

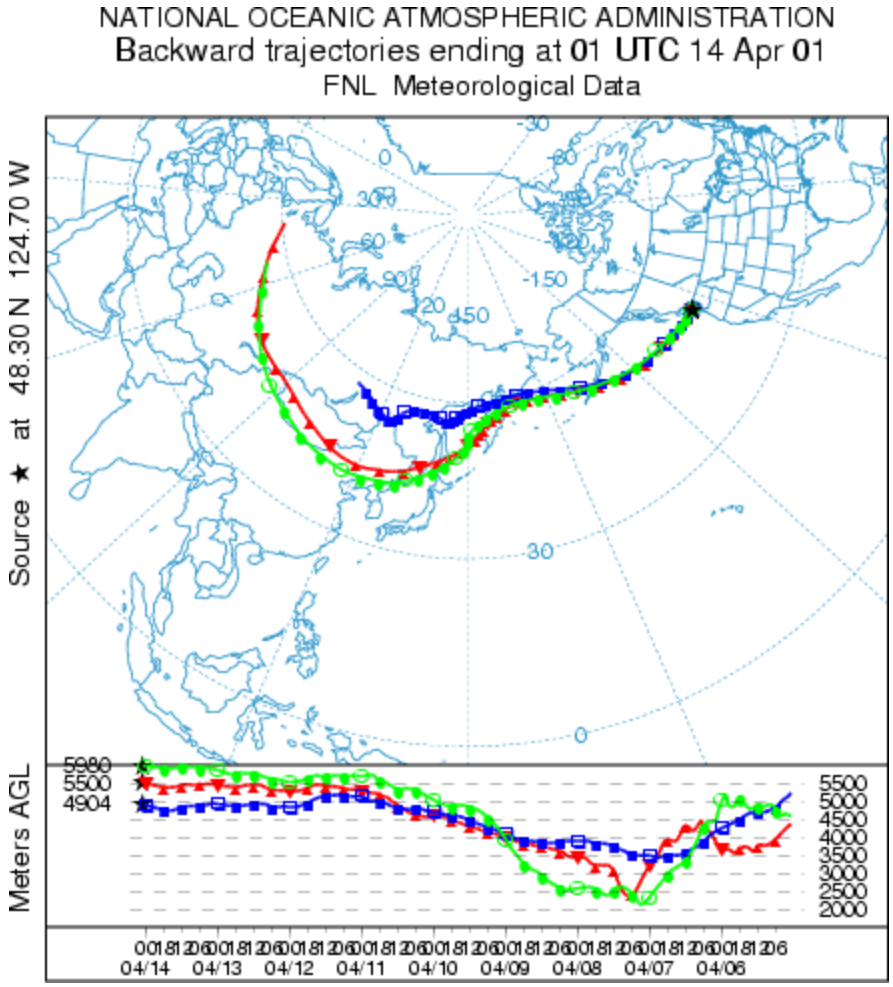

Figure 7. Mean sea level pressure on April 8.

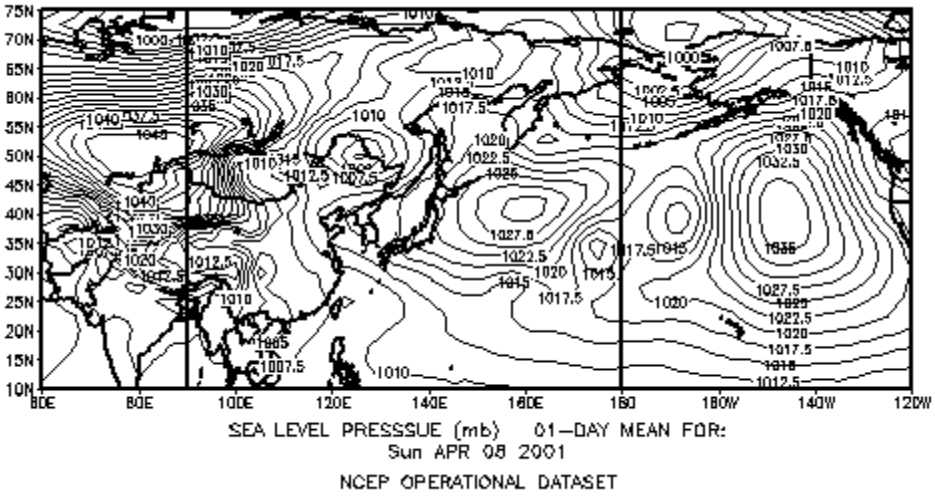

Figure 8. Spring 2001 marine mean ± 1σ and second data from flight 9 on April 25, 2001. NMHCs and CO are from 5-minute canister samples.

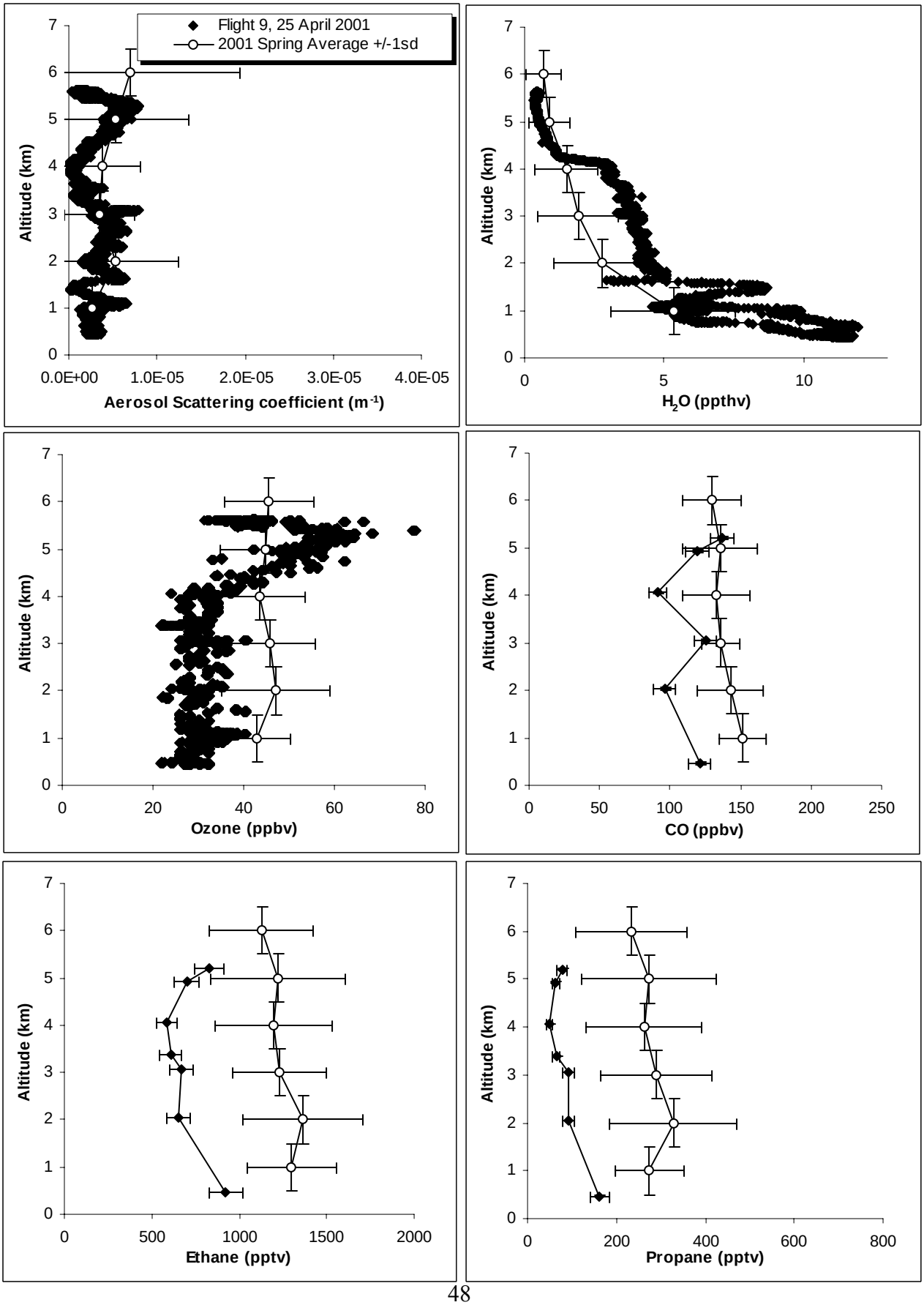

Figure 9. NOAA HYSPLIT READY 10day backward trajectory arriving on April 25, 2001at 0-6km

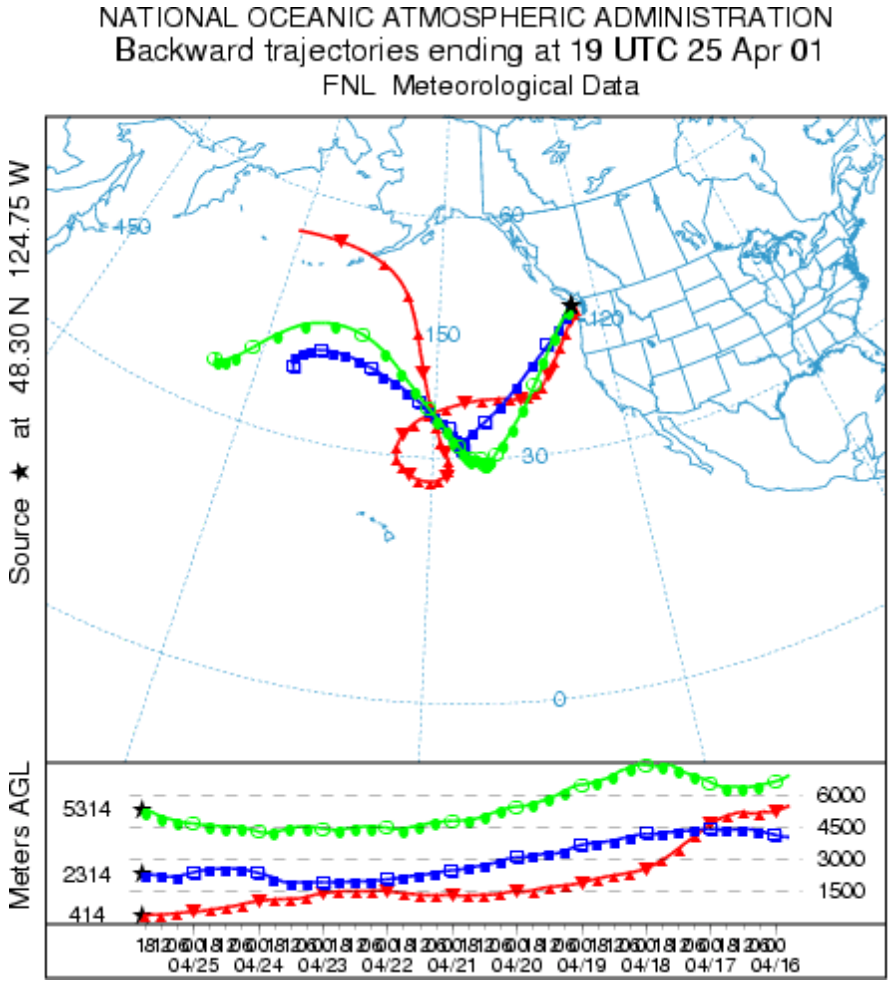

Figure 10. Spring 2001 marine mean ± 1σ and second data from flight 12 on May 6, 2001. NMHCs and CO are from 5-minute canister samples.

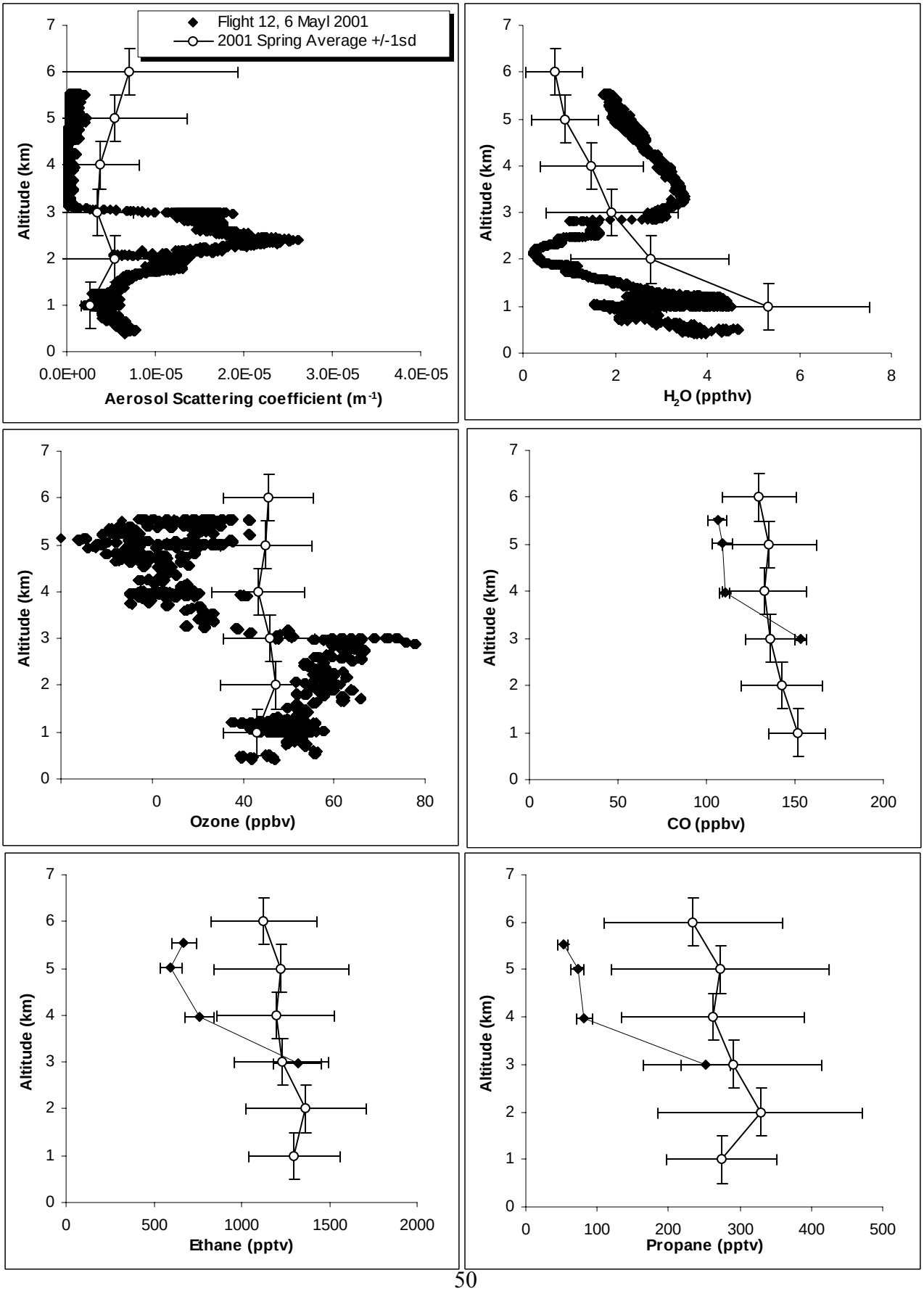

Figure 11. NOAA HYSPLIT READY 10day backward trajectory arriving May 6, 2001 at 1.5-3.5 km.

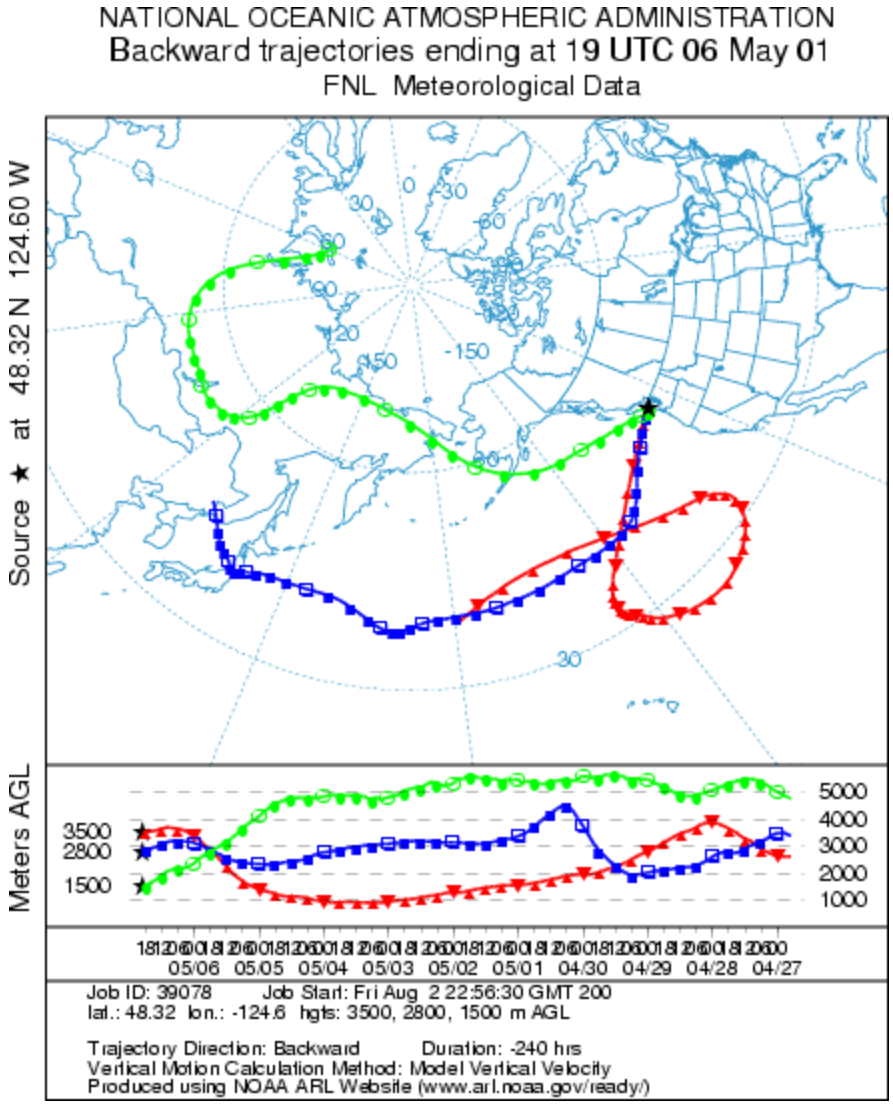

Plate 1a. TOMS Satellite Image Aerosol Index on (a) 8 April 2001 and (b) 14 April 2001.

a.

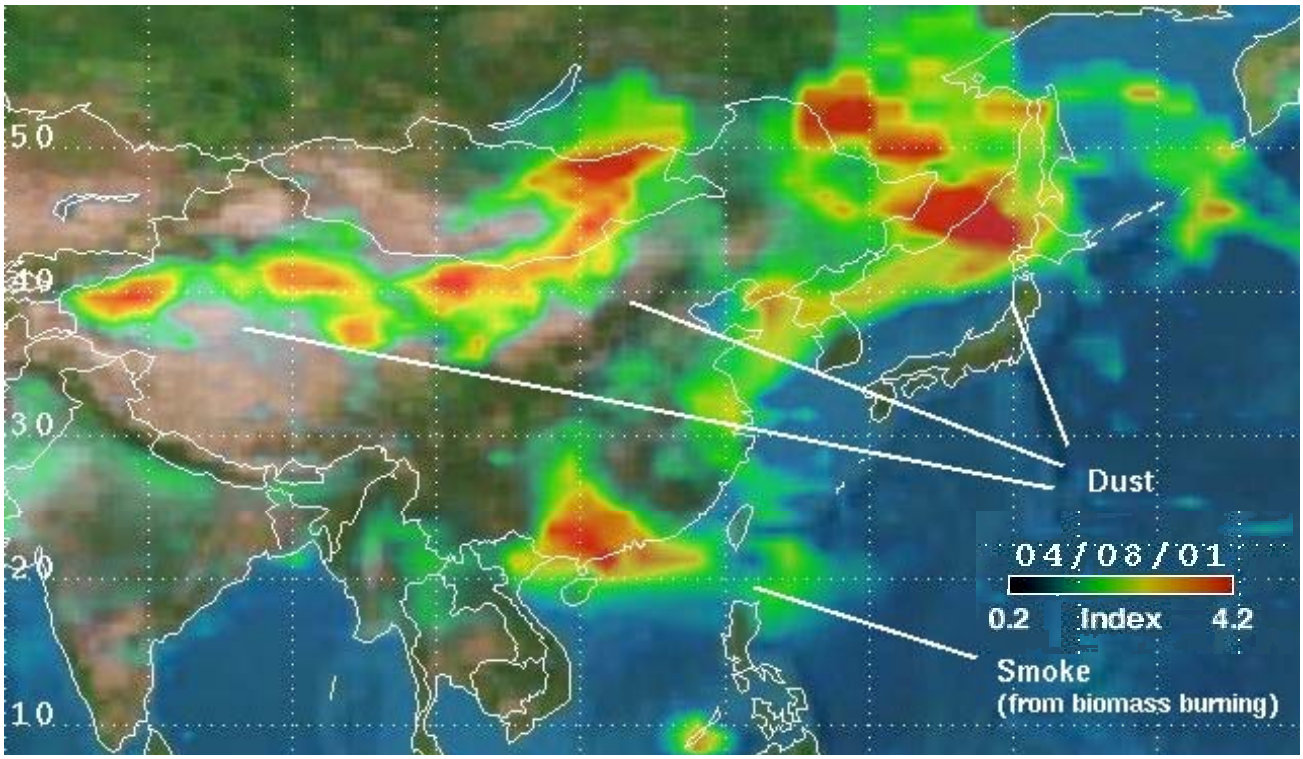

Plate 1b. TOMS Satellite image Aerosol Index on April 14, 2001.

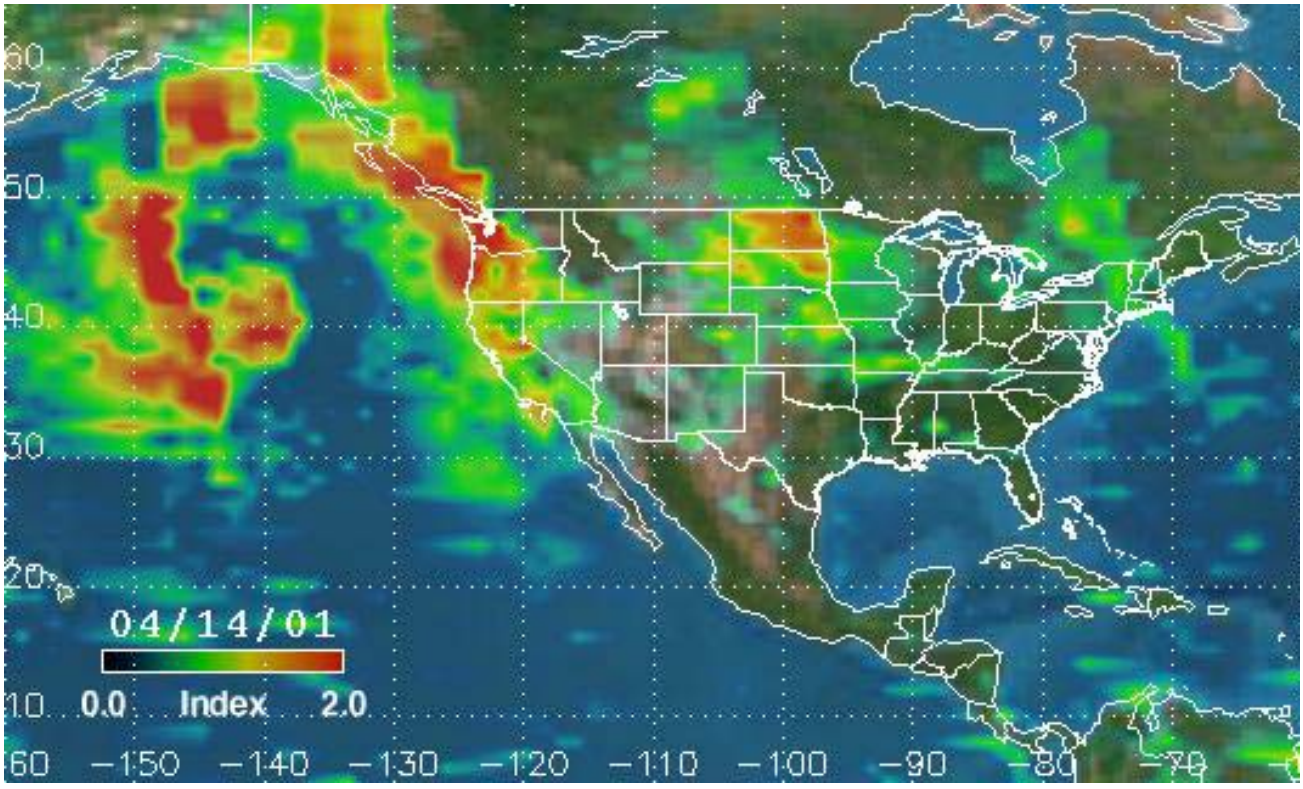

Figure A1. Ångstrom Exponent.